Cellular Microbiology (2015) **17**(5), 666–687
doi:10.1111/cmi.12391
First published online 25 November 2014

Yersinia pestis targets neutrophils via complement receptor 3

Peter M. Merritt,[1] Thomas Nero,[1] Lesley Bohman,[1] Suleyman Felek,[2†] Eric S. Krukonis[3] and Melanie M. Marketon[1*]

[1]*Department of Biology, Indiana University, Bloomington, IN, USA.*

[2]*Department of Biologic and Materials Sciences, University of Michigan School of Dentistry, Ann Arbor, MI, USA.*

[3]*Department of Biomedical and Diagnostic Sciences, University of Detroit Mercy School of Dentistry, Detroit, MI, USA.*

Summary

***Yersinia* species display a tropism for lymphoid tissues during infection, and the bacteria select innate immune cells for delivery of cytotoxic effectors by the type III secretion system. Yet, the mechanism for target cell selection remains a mystery. Here we investigate the interaction of *Yersinia pestis* with murine splenocytes to identify factors that participate in the targeting process. We find that interactions with primary immune cells rely on multiple factors. First, the bacterial adhesin Ail is required for efficient targeting of neutrophils *in vivo*. However, Ail does not appear to directly mediate binding to a specific cell type. Instead, we find that host serum factors direct *Y. pestis* to specific innate immune cells, particularly neutrophils. Importantly, specificity towards neutrophils was increased in the absence of bacterial adhesins because of reduced targeting of other cell types, but this phenotype was only visible in the presence of mouse serum. Addition of antibodies against complement receptor 3 and CD14 blocked target cell selection, suggesting that a combination of host factors participate in steering bacteria towards neutrophils during plague infection.**

Received 6 September, 2014; revised 18 October, 2014; accepted 28 October, 2014. *For correspondence. E-mail mmarketo@indiana.edu; Tel. (+1) 812 856 3198; Fax (+1) 812 855 6705.
†Present address: Department of Medicine, Richmond University Medical Center, Staten Island, NY, USA.

Introduction

Many bacteria assemble nanomachines on their surfaces to deliver protein cargo to specific destinations. In Gram-negative bacteria, type III secretion systems (T3SS) are often engaged to deliver bacterial proteins into eukaryotic cells in a process that involves assembly of a needle-like structure on the bacterial surface (Buttner, 2012). The pathogenic *Yersinia* species (*Y. pestis*, *Y. pseudotuberculosis* and *Y. enterocolitica*) rely on a plasmid-encoded T3SS to deliver a suite of effectors, known as Yops, into immune cells (Dewoody *et al.*, 2013). The T3SS is an essential virulence factor for *Yersinia spp.* and many of the Yops function to disarm the host defences by inhibiting phagocytosis, inducing apoptosis, and modulating the inflammatory response (Viboud and Bliska, 2005; Ruckdeschel *et al.*, 2008). Despite sharing a highly conserved T3SS and set of Yop effectors, the three pathogenic *Yersinia* spp. manifest distinctly different diseases. *Y. enterocolitica* and *Y. pseudotuberculosis* are found in soil and water, and upon ingestion they typically cause self-limiting gastroenteritis (Galindo *et al.*, 2011). In the mouse model of infection, these bacteria will colonize Peyer's patches and mesenteric lymph nodes, followed by dissemination to the spleen and liver. On the other hand, *Y. pestis* is the causative agent of bubonic plague, which is a vector-borne disease that is maintained in rodent reservoirs (Perry and Fetherston, 1997; Gage and Kosoy, 2005). Once delivered to a mammalian host by fleabite, the bacteria colonize the draining lymph node where bacterial replication leads to the characteristic inflamed, painful bubo. Subsequently, bacteria disseminate to more distant lymph nodes as well as spleen and liver (Sebbane *et al.*, 2005).

Although disease progression is different for enteric *Yersinia* compared with *Y. pestis*, all three species share a tropism for lymphoid tissue. Investigating the nature of bacterial interaction with primary cells *in vivo* has been made possible by recent technological advancements. Using β-lactamase fused to a Yop effector, which is delivered in a T3SS-dependent manner, Yop injection into host cells can be detected by flow cytometry (Charpentier and Oswald, 2004; Marketon *et al.*, 2005; Koberle *et al.*, 2009; Durand *et al.*, 2010). With this approach, it was shown that *Y. pestis* selects certain immune cells for injection of Yops *in vivo*, particularly innate immune cells (neutrophils, dendritic cells and

macrophages; Marketon *et al*., 2005; Pechous *et al*., 2013). A similar preference for phagocytes was observed in spleens from mice infected with *Y. enterocolitica* and *Y. pseudotuberculosis* (Koberle *et al*., 2009; Durand *et al*., 2010). More recently, a biphasic response was demonstrated in lung tissue, whereby alveolar macrophages are targeted early in infection followed by preferential targeting of neutrophils in the later stages of infection by both *Y. pestis* and *Y. pseudotuberculosis* (Pechous *et al*., 2013; Paczosa *et al*., 2014). At present, the mechanism that promotes *Yersinia* preference for neutrophils and other phagocytes *in vivo* is unknown; however, at least for the enteric *Yersinia*, this preference appears to be maintained during *in vitro* infections of homogenized tissues (Koberle *et al*., 2009; Durand *et al*., 2010; Paczosa *et al*., 2014), which indicates that cell preference is not simply dictated by bacteria becoming surrounded and confined in tissues by infiltrating phagocytes. Rather, the data suggest that some type of receptor–ligand interaction should mediate the bacterial preference for certain cell types.

Several bacterial adhesins have been shown to mediate attachment of *Yersinia* to mammalian host cells. In the enteric *Yersinia*, Ail, YadA and invasin play a prominent role in adhesion, and correspondingly mutants lacking these genes manifest defects in colonization and dissemination during *in vivo* infections (Miller and Falkow, 1988; Pepe *et al*., 1995; Marra and Isberg, 1997; Handley *et al*., 2005; Durand *et al*., 2010; Uliczka *et al*., 2011; Paczosa *et al*., 2014). Adhesion to host cells is necessary for injection of Yop effectors, and in the absence of these adhesins, Yop delivery is compromised (Kapperud *et al*., 1985; 1987; Bliska *et al*., 1993; Durand *et al*., 2010; Maldonado-Arocho *et al*., 2013; Paczosa *et al*., 2014). In particular, Ail and YadA are required for Yop translocation in lungs of infected mice (Paczosa *et al*., 2014), whereas YadA, invasin and Ail each contribute to translocation in spleens of infected mice in a strain-dependent manner, depending on the relative expression levels of each adhesin (Maldonado-Arocho *et al*., 2013). In addition to their roles as adhesins, YadA and Ail also facilitate resistance to serum-mediated bacterial lysis (Pierson and Falkow, 1993; Biedzka-Sarek *et al*., 2005; Leo and Skurnik, 2011; Ho *et al*., 2012a; Schindler *et al*., 2012). Furthermore, Ail and YadA counteract the effects of complement, probably by inhibiting opsonophagocytosis, to allow dissemination and growth in the spleen (Maldonado-Arocho *et al*., 2013; Paczosa *et al*., 2014).

Despite their importance to pathogenesis of enteric *Yersinia*, neither YadA nor invasin is expressed by *Y. pestis*. Instead, the predominant *Y. pestis* adhesins appear to be Ail, Pla and PsaA (pH6 antigen; Felek and Krukonis, 2009; Felek *et al*., 2010). Ail and Pla are both outer membrane proteins, while the *psa* operon encodes a fimbrial structure. Pla, which is absent from the enteric *Yersinia*, is an outer membrane adhesin and protease that facilitates degradation of extracellular matrix proteins and promotes bacterial dissemination (Sodeinde *et al*., 1988; 1992). PsaA, also called MyfA, is present in all three *Yersinia* spp., but its expression is restricted to slightly acidic conditions at temperatures above 36°C (Ben-Efraim *et al*., 1961; Iriarte *et al*., 1993; Yang *et al*., 1996). Though Ail is present in all three *Yersinia* spp., its expression pattern and functionality differs. In *Y. pestis*, Ail is expressed at lower temperatures, but expression is optimal at 37°C at which point Ail makes up 20–30% of the outer membrane protein content (Kolodziejek *et al*., 2007; Bartra *et al*., 2008; Felek and Krukonis, 2009; Pieper *et al*., 2009). Besides conferring serum resistance, *Y. pestis* Ail mediates adhesion via binding to the extracellular matrix proteins laminin and fibronectin (Kolodziejek *et al*., 2007; Bartra *et al*., 2008; Tsang *et al*., 2010; Yamashita *et al*., 2011). This adhesive activity is important for the T3SS, and *Y. pestis* strains lacking Ail suffer from severely reduced Yop translocation (Felek and Krukonis, 2009; Felek *et al*., 2010). It is thought that the severe attenuation of Δ*ail* mutants in the rat model stems from the combined roles for Ail in coordinating serum resistance and cell adhesion (Hinnebusch *et al*., 2011).

Given that adhesins function to mediate interactions between bacteria and host cells, recent work has investigated the contribution of adhesins to *Yersinia* target cell preference. It was demonstrated that *Y. pseudotuberculosis* lacking the three major adhesins YadA, invasin and Ail was still capable of T3SS-dependent Yop injection, and that the preference for neutrophils among splenocytes was maintained, suggesting the possibility of adhesin-independent interactions (Maldonado-Arocho *et al*., 2013). Moreover, Maldonado-Arocho *et al*. showed that addition of serum to *ex vivo* splenocyte infections enhanced bacterial specificity for neutrophils (Maldonado-Arocho *et al*., 2013).

Here we have attempted to identify the factors that direct *Y. pestis* targeting of innate immune cells for Yop injection. We find that target cell preference is maintained during *ex vivo* infection of splenocytes, and that neutrophils are still the preferred cell type in the absence of organ architecture. In agreement with previous work using tissue culture infections (Felek *et al*., 2010), we find that Ail is the predominant adhesin-mediating efficient injection of murine splenocytes. In an attempt to identify factors conferring specificity to neutrophil targeting, we investigated the role of serum. Surprisingly, we found that mouse serum suppressed overall levels of Yop injection, which appears to be a consequence of increased specificity towards myeloid cells, neutrophils in

particular. Notably, we show that neutrophil targeting is mediated by complement receptor 3 and, to a lesser extent, CD14.

Results

Yops are translocated by the ail mutant in vivo

In light of the observations that Ail is important for mediating Yop delivery, and that the Δ*ail* mutant is severely attenuated *in vivo* (Felek and Krukonis, 2009), we wondered whether the virulence defect could be attributed to a lack of Yop injection *in vivo*. To address this, we employed the β-lactamase (Bla) reporter system that we previously developed for measuring T3SS injection of primary immune cells (Marketon *et al*., 2005; Houppert *et al*., 2013). In this assay, translocation (injection) of the YopM-Bla reporter is monitored via cleavage of the fluorescent dye CCF2-AM. CCF2-AM-stained cells fluoresce green upon excitation with violet light (405 nm). In the presence of Bla, the dye is cleaved resulting in a shift from green to blue fluorescence, depending on the amount of dye that is cleaved. Cells that have been injected with YopM-Bla will fluoresce blue. On the other hand, uninfected cells or cells infected with *Y. pestis* expressing GST-Bla (negative control) will fluoresce green. In combination with the immunophenotyping strategy outlined in Supporting Information Fig. S1, flow cytometry is used to identify cell types and determine which cells have been injected.

Mice were infected with wild-type (WT) KIM5, the Δ*ail* mutant, or a T3SS-mutant (*yscU*-) carrying either YopM-Bla or Gst-Bla. Importantly, the LD_{50} of the mutants are $\sim 1.7 \times 10^5$ colony-forming units (CFU) for Δ*ail* and $\geq 10^7$ CFU for Δ*yscU* compared with ~ 10 CFU for the KIM5 parent (Perry and Fetherston, 1997; Felek and Krukonis, 2009). To compensate for the virulence defects of the mutants and ensure recovery of similar bacterial loads from spleens during a 3-day time course, we used 100-fold higher inocula for the mutants (10^6 CFU compared with 10^4 CFU for WT). Infected spleens were then harvested, and the bacterial load was quantified as well as the percentage of splenocytes that were injected with the YopM-Bla reporter. Previous work indicated that while the parent KIM5 strain could be detected in the spleen 1 day post-infection, YopM-Bla injection was below the limit of detection (Marketon *et al*., 2005). We therefore began monitoring KIM5-infected mice on day 2 post-infection. As shown in Fig. 1A, the mean bacterial burden from KIM5-infected mice was $10^{5.35}$ CFU per spleen on day 2, and by day 3, there was a 1.5-log increase in the bacterial load ($P < 0.001$). Looking at the number of splenocytes injected with YopM-Bla during WT infection, about 1.1% of cells appeared blue on day 2 (Fig. 1B). These blue

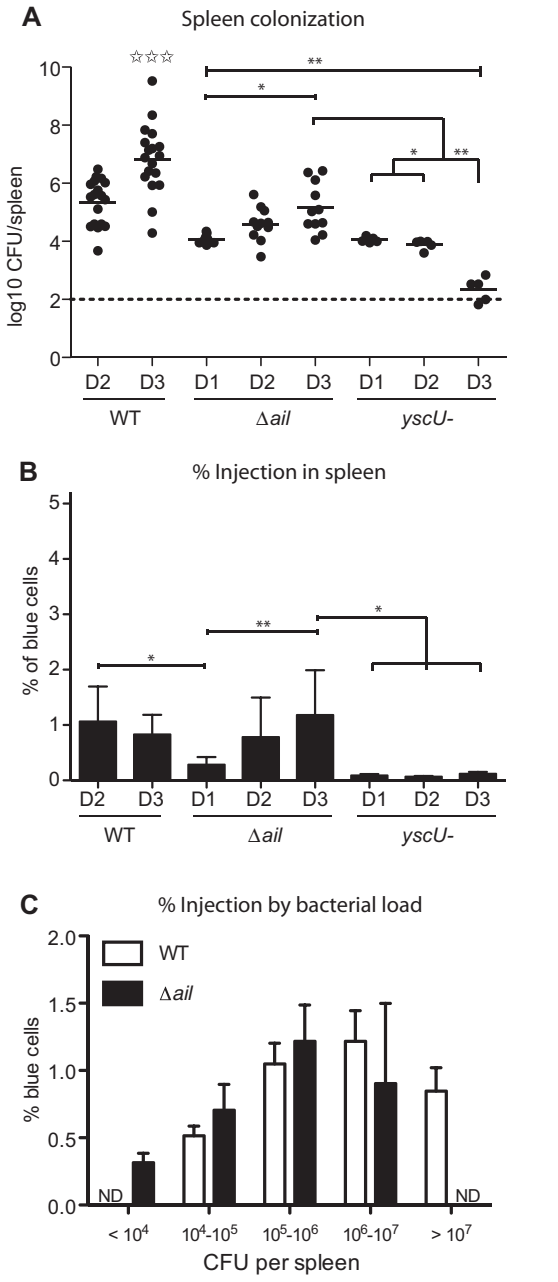

Fig. 1. The Δ*ail* mutant translocates Yops *in vivo*. Mice were infected with the indicated *Y. pestis* strains expressing either YopM-Bla or Gst-Bla. Spleens were harvested and homogenized at days 1, 2 and 3 post-infection. A portion of each homogenate was used to enumerate bacterial load (A). The remaining splenocyte suspension was stained with CCF2-AM and analysed by flow cytometry to quantify the number of blue (injected) cells (B). Data was analysed by one-way ANOVA with Tukey post-hoc test (*$P < 0.05$, **$P < 0.01$, ☆☆☆$P < 0.001$). Asterisks reflect indicated pair-wise comparisons. The stars indicate that WT colonization on day 3 was significantly higher than all other samples. While B shows % injection in infected spleens according to day post-infection, (C) shows the same data according to bacterial loads. ND indicates 'not determined' since only one mouse infected with the WT strain had a bacterial load below 10^4 CFU, and no mice infected with the Δ*ail* mutant had a bacterial load above 10^7 CFU (see A).

cells are indicative of T3SS-dependent injection of YopM-Bla, rather than phagocytosis of bacteria because infection with either WT expressing the Gst-Bla negative control (data not shown) or with the T3SS mutant (*yscU*$^-$) expressing YopM-Bla each yielded only ~0.08% blue cells. Despite the fact that bacterial burden of WT *Y. pestis* increased between days 2 and 3 of infection, the average number of YopM-Bla positive cells tended towards a slight reduction, though, this was not a statistically significant decrease. In contrast to WT, the Δ*ail* mutant showed a trend of increasing amounts of Yop injection as the infection progressed. The colonization levels of the Δ*ail* mutant were relatively stable with only a slight increase in the average bacterial burden from day 1 to day 3 (10^4 CFU vs. 10^5 CFU, respectively, $P < 0.05$). In fact, the bacterial loads of spleens from mice infected with the *ail* or *yscU* mutants on days 1 and 2 were not statistically different. Yet, despite the fairly low bacterial load for the Δ*ail* mutant, there was a dramatic increase in the percentage of injected splenocytes between days 1 and 2, and this level of injection was maintained through day 3.

Because there was a broad range of bacterial load in infected mice, particularly on day 3 post-infection, we chose to pool the data from all days and then categorize according to the bacterial loads using 1-log increments (Fig. 1C). In this way, the ability of the *ail* mutant to target immune cells can be compared with that of WT using data from comparable bacterial burdens. When viewed this way, the data indicates that the two strains delivered Yops into immune cells to a similar extent. Though not statistically significant, there appeared to be a trend of more blue cells as the bacterial load increased until a peak is reached at about 10^6 CFU, above which the number of blue cells decreased. When taken together, the data indicate that when the Δ*ail* mutant's colonization defect is compensated by a higher inoculum to achieve similar bacterial burdens, Yop delivery into splenocytes is comparable with WT *Y. pestis*.

We also evaluated whether recruitment of immune cells to the spleen is altered during infection by the Δ*ail* mutant. The data from WT infected animals (Supporting Information Fig. S2A) indicate that as the infection progressed and bacterial numbers increased, there was a corresponding increase in B-cells within spleens. In contrast, dendritic cells, macrophages and NK cells were significantly reduced as bacterial burden increased. As expected, there was an initial increase in the neutrophil population, but above 10^6 CFU, the number of neutrophils declined. As shown in Supporting Information Fig. S2B, infection by the Δ*ail* mutant yielded similar trends in the total splenocyte populations. Although the activation status of these cell types could differ, it appears that under these infection conditions, the Δ*ail* mutant encounters a similar overall distribution of splenocytes as does WT *Y. pestis*.

Ail contributes to efficient targeting of neutrophils in vivo

To analyse targeting of specific cell types for Yop injection, we evaluated three parameters: frequency of injection, distribution of injected cells and targeting efficiency. Figure 2 shows the analysis for mice infected with the WT strain; however, the general strategy for this analysis is described in Supporting Information Fig. S3 using a simpler dataset. Frequency of injection refers to the percentage of each cell type that is positive for the YopM-Bla reporter. As expected, all myeloid cell types were injected by WT at higher frequencies than were the lymphoid populations (Fig. 2A). In fact, relatively few lymphoid cells were targeted until late in infection (i.e. $> 10^7$ CFU). Importantly, the percentage of injected monocytes and neutrophils increased dramatically and significantly by about 10^6 CFU and then remained high as bacterial burden increased (Fig. 2A). Despite this persistent targeting of neutrophils at the highest bacterial loads, neutrophils represented only a small fraction of the total population of blue cells (Fig. 2B). This also corresponds to a drop in total neutrophils (Supporting Information Fig. S2A). Altogether, the trend shifted from injection of myeloid cells at lower bacterial loads towards injection of B-cells at $> 10^7$ CFU (Fig. 2B).

Because the myeloid cell types are a minor portion of the splenocyte population, and because the cell distribution changes during infection, we normalized the distribution data by dividing the distribution of injected cell types by the distribution of total cell types (injected + uninjected), resulting in a metric that we term 'targeting efficiency' (described in Supporting Information Fig. S3). Using this metric, we avoid bias in apparent target cell preferences that may stem from any fluctuations in the total numbers of individual cell types as a result of mouse-to-mouse variability or as a by-product of infection and cell death. A targeting efficiency value of 1 indicates no preference because the relative proportion of injected cells for a particular cell type represents the same proportion of that type within the total splenocyte mixture. Targeting efficiencies greater than one indicate an enrichment of the cell type within the injected cell population compared with the total cell population (a preference for those cells). Targeting efficiencies less than one indicates that those cell types are under-represented within the injected population, which could reflect active exclusion or avoidance of those cells by the bacteria. Importantly, B- and T-cells were not efficiently targeted during WT infection (Fig. 2C). In contrast, targeting efficiencies were extremely high for the myeloid populations, particularly neutrophils, monocytes and eosinophils.

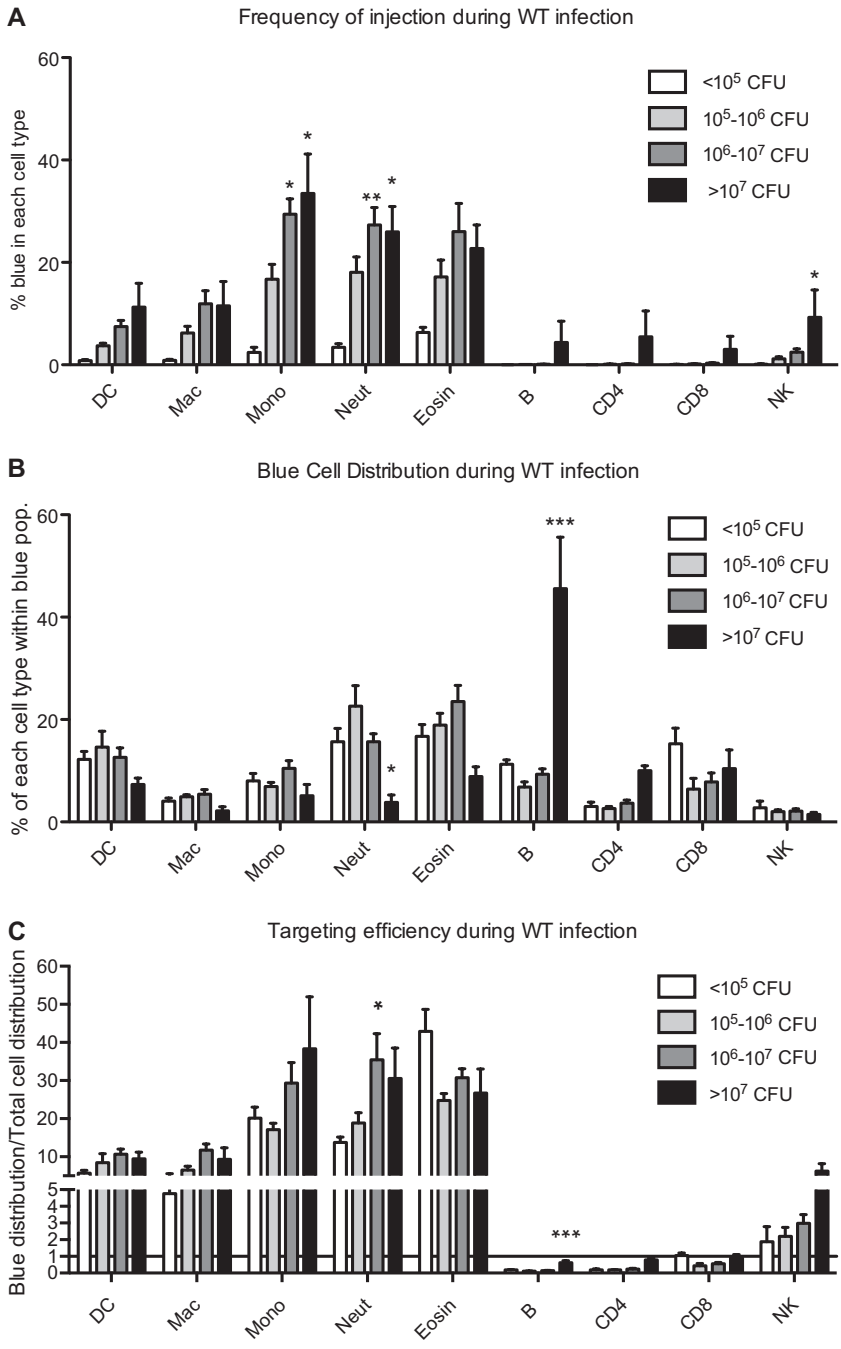

Fig. 2. Target cell selection during infection with WT *Y. pestis*. Mice described in Fig. 1 were infected with WT *Y. pestis*, and splenocytes were analysed by flow cytometry (described in Supporting Information Fig. S1) to identify each cell type as well as blue injected cells.
A. Frequency of injection. After cell types are identified from total live cells, the % of blue cells in each population was determined.
B. Blue cell distribution. Blue cells were first identified from total live cells and then subjected to the myeloid and lymphoid analysis to identify cell types within the blue population.
C. Targeting efficiency. The blue cell distribution was compared with the total cell distribution. The fold difference for each cell type is the 'targeting efficiency', and these values are graphed here (horizontal line at $Y = 1$ indicates no cell preference).
Data were analysed by two-way ANOVA with Bonferroni multiple comparisons test to determine significant differences between the lowest CFU load compared with higher CFU loads for each cell type ($^{*}P < 0.05$, $^{**}P < 0.01$, $^{***}P < 0.001$). DC, dendritic cells; Mac, macrophages; Mono, monocytes; Neut, neutrophils; Eosin, eosinophils; CD4, T helper cells; CD8, T cytotoxic cells; NK, NK cells.

The data in Fig. 2 indicates that neutrophils are a major target of Yop injection during WT infections. In contrast, targeting of neutrophils was less prominent during infections with the Δ*ail* mutant (Fig. 3). To facilitate the comparison of mutant vs WT data, Fig. 4 shows a side-by-side depiction of the data for the 10^5–10^6 CFU and 10^6–10^7 CFU categories for both strains. Most notable is the dramatic reduction in neutrophil targeting efficiency by the mutant compared with WT for both bacterial burden categories (Fig. 4B). Neutrophils as well as other myeloid cells were injected at frequencies higher than that of lymphoid cells (Fig. 3A). However, after an initial increase in injection levels, the percentages of injected cells for each myeloid cell type decreased as the bacterial loads increased beyond 10^6 CFU. Further distinguishing the mutant from WT is the distribution of the blue cell population (Fig. 3B). While myeloid cells represented a major portion of injected cells until very high bacterial loads during WT infection (Fig. 2B), there is no clear major population in the distribution of injected cells from mice

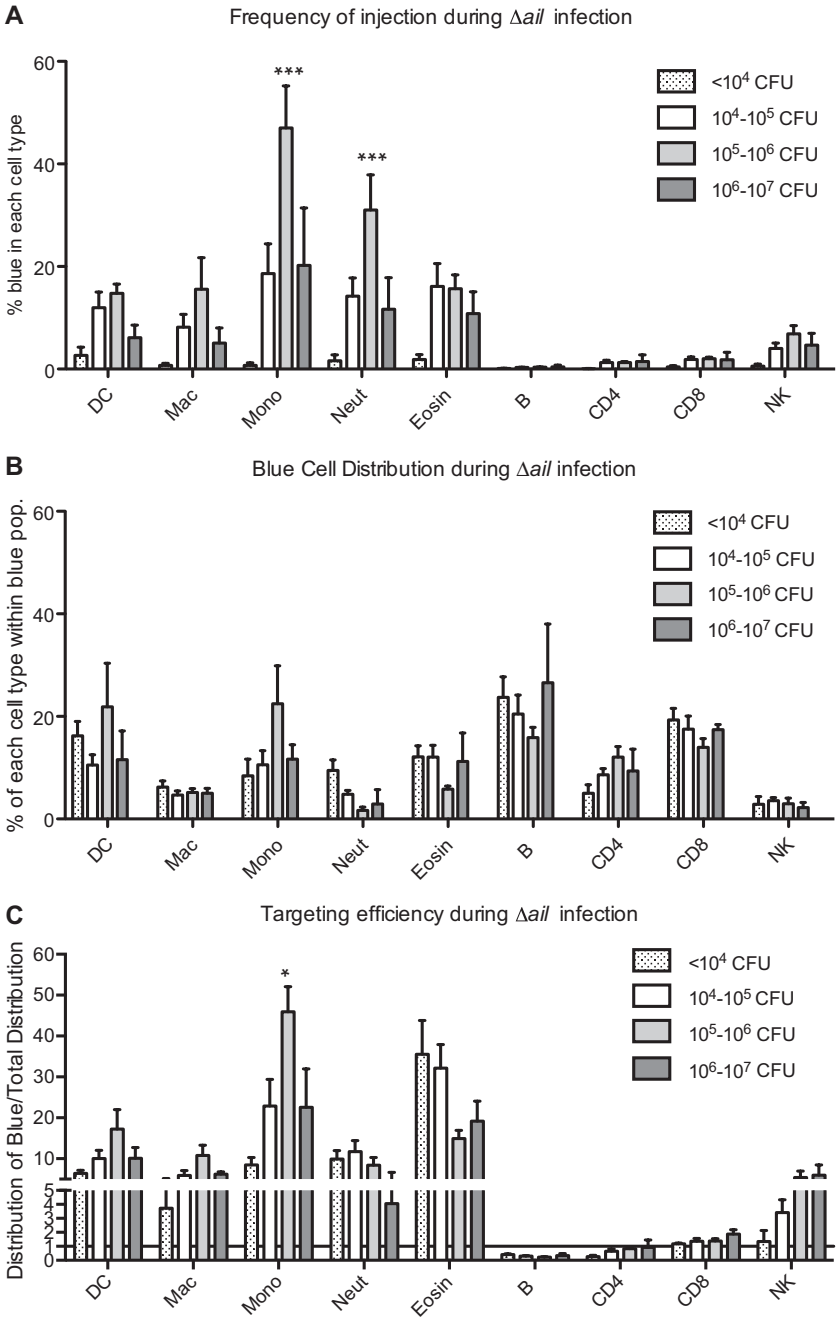

Fig. 3. Target cell selection during infection with *Δail Y. pestis*. Mice described in Fig. 1 were infected with *Δail Y. pestis*, and splenocytes were analysed as described in Supporting Information Fig. S1.
A. Frequency of injection.
B. Blue cell distribution.
C. Targeting efficiency.
Data were analysed by two-way ANOVA with Bonferroni multiple comparisons test to determine significant differences between the lowest CFU load compared with higher CFU loads for each cell type (*$P < 0.05$, ***$P < 0.001$). DC, dendritic cells; Mac, macrophages; Mono, monocytes; Neut, neutrophils; Eosin, eosinophils; CD4, T helper cells; CD8, T cytotoxic cells; NK, NK cells.

infected with the *Δail* mutant (Fig. 3B). Moreover, the targeting efficiencies for the myeloid cell types, particularly neutrophils, tended to be reduced compared with WT infections (Figs 3C and 4B).

Ex vivo *analysis of target cell selection during splenocyte infection*

The above data clearly indicate that Ail contributes to efficient Yop delivery into immune cells *in vivo*; however, interpretation of the role of Ail is complicated by the host immune response during infection. Therefore, to specifically address the contribution of Ail's adhesin activity to target cell selection, we used an *ex vivo* assay in which splenocyte suspensions from naive mice are used as a source of immune cells for *in vitro* infections (Houppert *et al.*, 2013). In this way, WT and mutant strains will have equal opportunity to interact with the same cell types. We identified the cell types using the same strategy described in Supporting Information Fig. S1. Again, we determined the frequency of injection, distribution of injected cells and targeting efficiency for each set of infections, as described

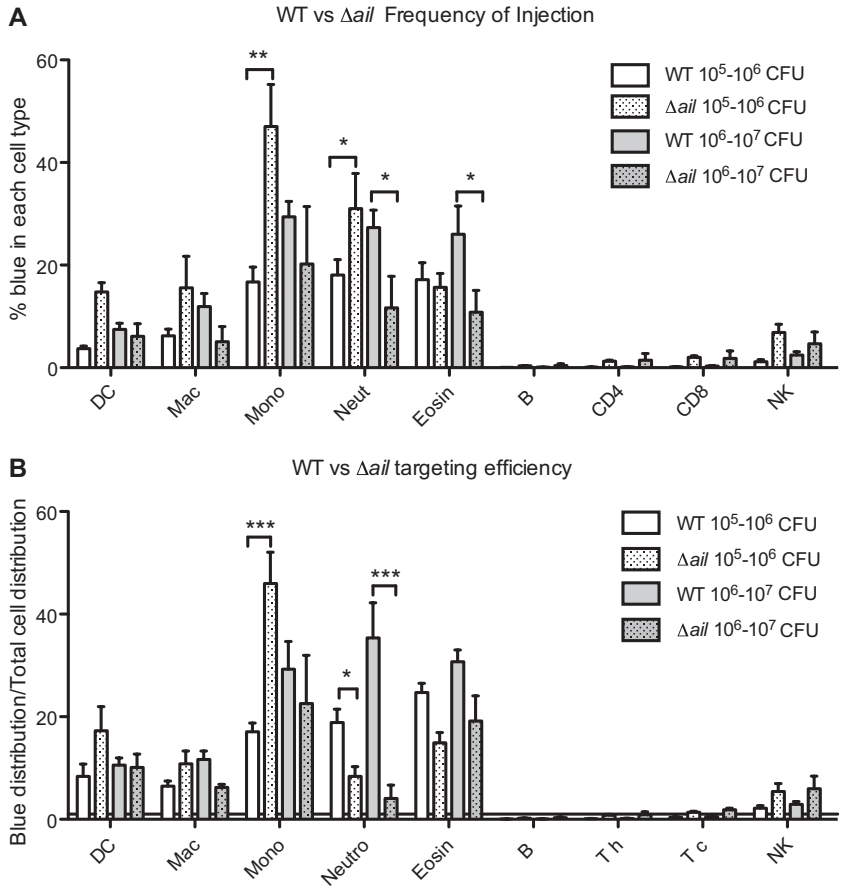

Fig. 4. Comparison of target cell selection during WT and *Δail* infections. Data shown in Figs 2 and 3 were graphed together to compare injection capabilities for each bacterial strain when bacterial loads were similar. Shown here are data from the 10^5–10^6 and 10^6–10^7 CFU categories.
A. Frequency of injection (% of each cell type that is blue).
B. Targeting efficiency (fold difference between the blue cell distribution vs the total distribution for each cell type).
Data were analysed by two-way ANOVA with Bonferroni multiple comparisons test to determine significant differences (*$P < 0.05$, **$P < 0.01$, ***$P < 0.001$). DC, dendritic cells; Mac, macrophages; Mono, monocytes; Neut, neutrophils; Eosin, eosinophils; CD4, T helper cells; CD8, T cytotoxic cells; NK, NK cells.

in Supporting Information Fig. S4. When splenocytes were infected with WT *Y. pestis*, the preference for myeloid cell types is readily apparent (Supporting Information Fig. S4A). More than 90% of the neutrophils had been injected, as well as more than 70% of dendritic cells and monocytes. Our data show that relatively few macrophages were injected (~ 17%), but that may be due to the fact that we excluded cells that are positive for the MHC class II marker in our analysis to facilitate identification of other cell types. It is possible that macrophages may become activated during the short ~ 1.5 h. infection, which may lead to MHC class II gene expression and a corresponding under-representation of macrophages in our assay. Interestingly, 46% of eosinophils were positive for YopM-Bla injection. The significance of possible eosinophil targeting during infection has not been addressed previously and may warrant future investigation. We also found that the majority of B-cells were also injected, but very few T-cells or NK cells were injected. The observation that B-cells can be injected agrees with previous data (Marketon *et al.*, 2005) showing that B-cells can be targeted by *Y. pestis in vitro*, but this is in contrast to *in vivo* data (Fig. 2A and Marketon *et al.*, 2005). Nevertheless, similar patterns of target cell preference were observed during *ex vivo* infections using *Y. enterocolitica* and *Y. pseudotuberculosis* (Koberle *et al.*, 2009; Durand *et al.*, 2010). Therefore, the *Yersinia* spp. appears to share the ability to target myeloid cells and B-cells *ex vivo*.

Although nearly all neutrophils (and other myeloid cells) were injected during *Y. pestis* infection, this represents only a small percentage of the total population of injected cells (Supporting Information Fig. S4B). In contrast, because B-cells are a major portion of the spleen, they correspondingly represent a major portion of the total population of injected cells. When targeting efficiency is evaluated for WT infection (Supporting Information Fig. S4E), it is clear that myeloid cells and B-cells are preferred targets, while T-cells and NK cells appear to be excluded.

Mouse serum influences Yop injection and reveals a role for Ail

We next wanted to address the potential role of bacterial adhesins, particularly Ail, in target cell selection. Towards that end, *ex vivo* assays were performed with WT, *Δail*, *Δpla/psaA* or the *Δail/pla/psaA* triple mutant. To our surprise, initial experiments revealed no profound differences

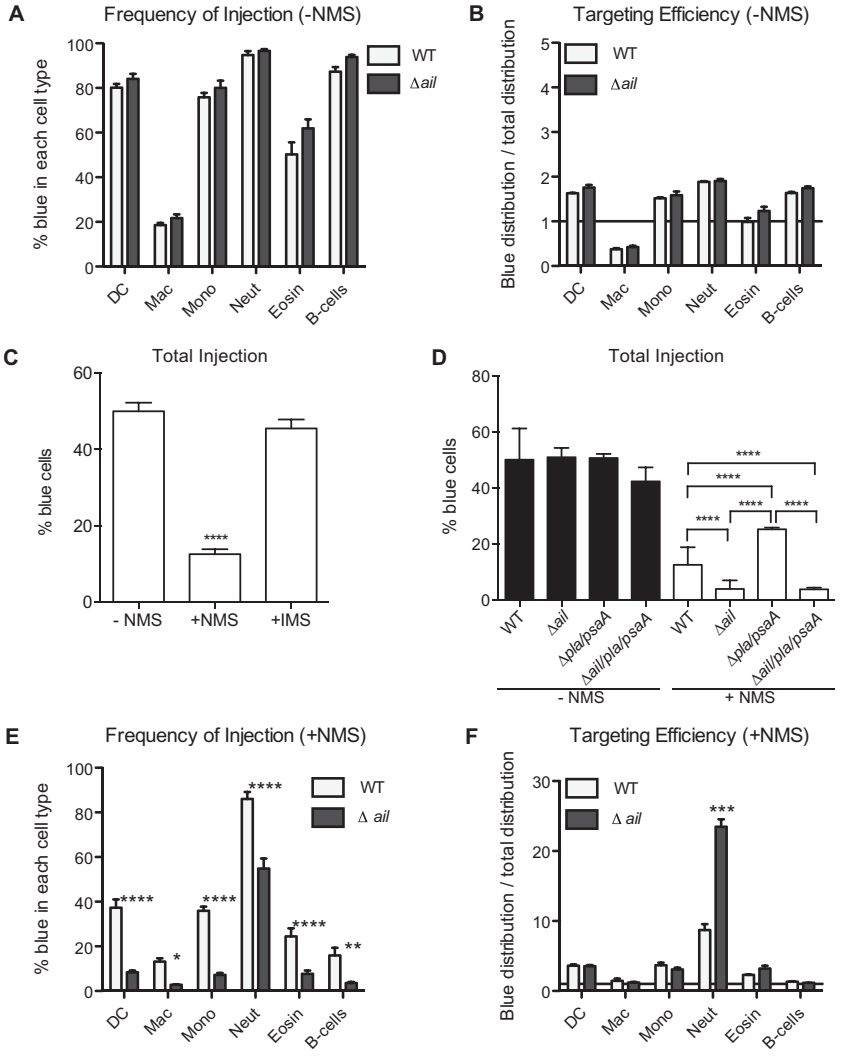

Fig. 5. A role for adhesins in the presence of mouse serum. Splenocytes from naive mice were infected at an MOI of 1 with the indicated *Y. pestis* strains expressing YopM-Bla or Gst-Bla (not shown). Infections were performed in RPMI containing FBS and cytochalasin D for 1.5 h. Where indicated, the medium was supplemented with 10% NMS or heat-IMS. Cells were stained with CCF2-AM and then analysed by flow cytometry.
A. The percentage of blue cells for individual cell types is shown for infections lacking NMS.
B. The targeting efficiency for each cell type is shown for infections lacking NMS. Horizontal line at Y = 1 indicates no cell preference.
C. Infections with WT *Y. pestis* were performed in the presence or absence of NMS or IMS. The percentage of blue cells in the total splenocyte population for each infection is shown. Data were analyzed using 1-way ANOVA with Dunnett multiple comparisons test (control = no serum).
D. The percentage of blue cells in the total splenocyte population for each infection is shown. Data were analyzed using 1-way ANOVA with Bonferroni multiple comparisons test (****$P < 0.0001$).
E. The percentage of blue cells for individual cell types is shown for infections containing NMS.
F. The targeting efficiency for each cell type is shown for infections containing NMS. Horizontal line at Y = 1 indicates no cell preference.
Data in panels A–B and E–F were analyzed by two-way ANOVA with Bonferroni multiple comparisons test to determine significant differences for each cell type infected with WT compared with the mutant. (*$P < 0.05$, **$P < 0.01$, ***$P < 0.0001$, ****$P < 0.0001$) DC, dendritic cells; Mac, macrophages; Mono, monocytes; Neut, neutrophils; Eosin, eosinophils.

between WT and any mutant (Fig. 5A and B and Supporting Information Fig. S5). However, we wondered if the conditions in the *ex vivo* assays might preclude observation of a targeting defect by the adhesin mutants. Since splenocytes are homogenized and rinsed prior to infection, there could be a soluble serum factor that is required for adhesin-mediated specificity and is missing or in low abundance. We therefore asked whether adding mouse serum to our *ex vivo* infection assay would influence targeting and would thereby reveal mutant deficiencies. Figure 5C shows the results of infecting murine splenocytes in the presence of either 10% normal mouse serum (NMS) or heat-inactivated mouse serum (IMS). Contrary to our expectations, addition of NMS significantly reduced overall injection. The suppressive effect of NMS appears to rely on heat-labile factors because adding IMS to the infections had no effect. Moreover, in the presence of NMS, the Δ*ail* mutant displayed reduced levels of injection compared with WT (Fig. 5D). To our surprise, the Δ*pla/psaA* mutant gave rise to significantly more injected cells compared with the WT infection. That phenotype seems to be dependent on Ail because with the triple mutant (Δ*ail/pla/psaA*), the frequency of injection was identical to that of the single Δ*ail* mutant. Together, these experiments indicate that Ail appears to be necessary for efficient Yop injection into splenocytes in the presence of serum, and suggest the possibility that Pla opposes Ail's adhesin activity.

Mouse serum enhances neutrophil targeting

Since addition of mouse serum reduced the total number of injected splenocytes, we investigated whether the phenomenon correlated with any changes to target cell selection. When splenocytes in the presence of 10% NMS were infected with WT *Y. pestis*, we observed significantly fewer ($P < 0.0001$) injected B-cells, dendritic cells, monocytes and eosinophils (Fig. 5E, white bars)

compared with infections performed in the absence of NMS (Fig. 5A, white bars). The frequency of injection was reduced ~ 50% for dendritic cells, monocytes and eosinophils, whereas for B-cells, the frequency of injection was reduced by ~ 75%. In contrast, neutrophil injection was unaffected as nearly all neutrophils were targeted for Yop injection in both conditions. This maintenance of neutrophil targeting in the midst of reduced targeting of other cell types correlates with ~ 10-fold higher targeting efficiency for neutrophils in the presence of NMS (Fig. 5F, white bars) compared with conditions lacking NMS (Fig. 5B, white bars). Thus, it appears that one or more heat-labile serum factors facilitate neutrophil targeting.

Ail is required for efficient injection of splenocytes

To investigate the nature of the injection defect for the Δ*ail* mutant seen in Fig. 5D, we analysed the immune cell populations to determine whether there was a change in target cell selection. In the presence of serum, there were significant decreases in the frequency of injection by the Δ*ail* mutant for B-cells and all myeloid populations except macrophages, though even macrophages followed the same trend (Fig. 5E, black bars). Injection of T-cells and NK cells was not significantly affected, since they were still not targeted to any appreciable extent (data not shown). Although there were fewer neutrophils injected by the Δ*ail* mutant, the magnitude of this decrease was less than that of other cell types. Therefore, neutrophils represent a larger fraction of the total injected population in Δ*ail* mutant infection, which correlates to a dramatic increase in the targeting efficiency of neutrophils for the Δ*ail* mutant compared with WT (Fig. 5F). Importantly, none of the targeting defects were observed for the Δ*ail* mutant in the absence of NMS (Fig. 5B). Therefore, we conclude that the adhesin-dependent phenotype is also serum-dependent.

Pla counteracts Ail activity

The data in Fig. 5D indicate that the Δ*pla/psaA* mutant injected YopM-Bla into more splenocytes than did WT *Y. pestis*. This is unexpected because Pla contributes to efficient injection of various tissue culture cell lines (Felek *et al*., 2010). To determine whether the target cell specificity is altered by the lack of Pla, we analysed the pattern of translocation into immune cell populations during infection with the Δ*pla/psaA* mutant. Supporting Information Figure S6A shows that most of the increase stems from injection of ~ 50% more B-cells by the mutant (black bars) compared with WT (white bars). Injection of dendritic cells and monocytes was also significantly increased. Notably, there was still no significant increase in targeting of T-cells or NK cells. Moreover, neutrophil targeting remained unaffected. Because the amount of injected neutrophils did not change, while other populations experienced higher frequencies of injection by the Δ*pla/psaA* mutant, this means that neutrophils represent less of the total population of injected cells. Correspondingly, there was a significant reduction in the neutrophil targeting efficiency for the Δ*pla/psaA* mutant compared with WT (Supporting Information Fig. S6B). However, these phenotypes were completely reversed when *ail* was deleted, as the triple Δ*ail/pla/psaA* mutant phenotype resembled that of the single Δ*ail* mutant (Supporting Information Fig. S6C and D). These data suggest that when only Ail is present (as in the Δ*pla/psaA* mutant), neutrophil targeting still occurs but there appears to be more interaction with the other preferred cell types (other myeloid cells and B-cells), thereby detracting from neutrophil interactions. However, in the absence of Ail, the preference for B-cells and myeloid cells over T-cells and NK cells is maintained. Moreover, this target cell selection is maintained during infection with a triple mutant lacking all three major adhesins, Ail, Pla and PsaA. These observations raise the possibility that both adhesin-dependent and -independent processes mediate target cell selection.

Bacterial adhesion to splenocytes

Throughout our experiments, we have consistently seen that T-cells and NK cells are not selected as targets for Yop injection, regardless of the experimental conditions. Moreover, we have seen fluctuations in the extent to which the bacteria target the preferred cell types. Therefore, we investigated whether these observations correlate with bacterial binding to host cells. To that end, we introduced a plasmid expressing a GFP variant (GFPuv) into *Y. pestis* WT and Δ*ail* mutant strains and then performed standard *ex vivo* infections of splenocytes in the presence or absence of serum. Using flow cytometry, we analysed bacterial adhesion by measuring the percentage of each cell type that was positive for GFP. Importantly, cytochalasin D was included in all *ex vivo* assays to prevent phagocytosis of attached bacteria. As shown in Supporting Information Fig. S7A, there was ≥ 50% bacterial adherence under all conditions. In the absence of serum, the Δ*ail* mutant was associated with more cells than was WT *Y. pestis* (61% compared with 53%). Addition of serum led to slightly reduced adhesion for both strains, and this effect was abrogated by heat inactivating the serum. To determine whether target cell selection for Yop injection correlates with bacterial adhesion, we identified which cells were GFP positive (Supporting Information Fig. S7B–D). Surprisingly, we found that most cell types had equivalent levels of GFP+ cells (~ 50% of the population), though there was a higher

frequency of GFP+ cells for neutrophils, monocytes and eosinophils, and this was true for both WT and Δ*ail* mutant infections (Supporting Information Fig. S7B). The effect of adding NMS to infections (Supporting Information Fig. S7A) correlated with reduced adhesion to B-cells for both WT and the *ail* mutant (Supporting Information Fig. S7C and D). Taking into account all the data in Supporting Information Fig. S7, the fact that nearly 100% of neutrophils were GFP+ agrees well with the fact that nearly all neutrophils become targets for Yop injection. However, the correlation does not extend to other cell types. For example, T-cells and NK cells show equivalent bacterial adhesion compared with B-cells, yet they do not appear to become T3SS targets. Thus, a lack of Yop injection by *Y. pestis* is not simply because of a lack of bacterial adhesion.

Contribution of host factors to target cell selection

Because there is an adhesin-independent phenomenon that contributes to neutrophil targeting (Fig. 5E and F and Supporting Information Fig. S6C and D), we investigated serum factors as potential specificity determinants. Since neutrophil targeting is compromised by heat inactivating serum, we assumed that some component of complement might be involved. We therefore attempted to rule out a role for antibody-mediated opsonization in target cell selection using two approaches. First, we used Protein A/G beads to deplete antibodies from serum, and then analysed whether target cell selection was affected. We did not see any differences in targeting during infection with either the WT or Δ*ail* mutant (data not shown). Second, we used Fc Block (anti-CD16/CD32) to block antibody Fc receptors on splenocytes prior to infection. Once again, this treatment had no affect on targeting during *ex vivo* infections (data not shown).

We then considered whether complement and/or other serum components were responsible for neutrophil targeting, keeping in mind that multiple factors may be at play. For example, lipopolysaccharide (LPS)-binding protein (LBP) is a soluble serum factor known to opsonize bacteria and mediate interactions with CD14 (Wright *et al.*, 1989; Grunwald *et al.*, 1996). Moreover, LcrV, a secreted T3SS component, has reported interactions with CD14 and TLR2 (Sing *et al.*, 2002; Abramov *et al.*, 2007), and recently, Ail was shown to bind C4b-binding protein (C4BP), Factor H and the complement proteins C4, C4b, C3b (Ho *et al.*, 2012a,b; 2014). In addition, the alternative pathway for complement activation could yield C3b opsonization. Concomitant Ail binding to Factor H would accelerate Factor I-mediated cleavage of C3b to iC3b, which is a primary ligand for CR3 and to a lesser extent CR4 (Sengelov, 1995; Blom *et al.*, 2003; Ho *et al.*, 2012b; 2014). Therefore, it is possible that target cell selection arises from a combination of interactions between the bacteria and host cells.

Since neutrophils are primary targets during *Y. pestis* infection, we attempted to narrow down the candidates by first considering which receptors might be enriched on neutrophils. To that end, we surveyed the expression of CD11b (for CR3), CD11c (for CR4), CD14 and TLR2 on splenocytes incubated in medium containing NMS (Fig. 6). As expected, most of the myeloid cells expressed CD11b, in contrast to B-cells (frequency indicated by white bars); however, the expression level (mean fluorescence intensity, MFI, indicated by black bars) was highest in neutrophils (Fig. 6A). On the other hand, expression of CD11c appeared to be most frequent and strongest in dendritic cells (Fig. 6B). Interestingly, we found that CD14 was highly enriched in neutrophils, as ~ 60% of the population was CD14+ and also expressed high levels per cell (Fig. 6C). TLR2 was found on most of the neutrophils, and to a lesser extent on other myeloid cells and B-cells; however, expression level per cell was highest in neutrophils (Fig. 6D).

Neutrophil targeting is mediated by host factors

To investigate the possibility of multiple or complex interactions between *Y. pestis* and target cells, we attempted to block target cell selection by pretreating splenocytes with several antibodies, either alone or in combination, prior to infection. We then performed *ex vivo* infections in the presence or absence of NMS using WT *Y. pestis* and the Δ*ail/pla/psaA* mutant. If the pretreatments inhibit serum-dependent binding, then targeting should be adhesin dependent and should be observed during infection with WT but not the triple adhesin mutant. We chose to use anti-CD11b and anti-CD11c to block CR3 and CR4 respectively. We chose anti-CD14 to block multiple possible routes of interaction (via LBP, TLR2, TLR4), since CD14 is a common facilitator of those pathways. As expected, pretreatment with the antibody cocktail in the absence of NMS had no effect on target cell selection during infection with either WT or the triple adhesin mutant (Supporting Information Fig. S8). In contrast, the antibody cocktail led to a dramatic reduction of neutrophil targeting in the presence of NMS (Supporting Information Fig. S8). We then compared the ability of either WT *Y. pestis* or the triple adhesin mutant to target neutrophils in the presence of both NMS and the antibody cocktail (Fig. 7). We found that the antibodies significantly reduced the percentage of both monocytes and neutrophils that were injected by WT (Fig. 7A), and this led to a corresponding drop in targeting efficiency for both cell types (Fig. 7B). For the adhesin mutant, antibody pretreatment nearly abolished injection of

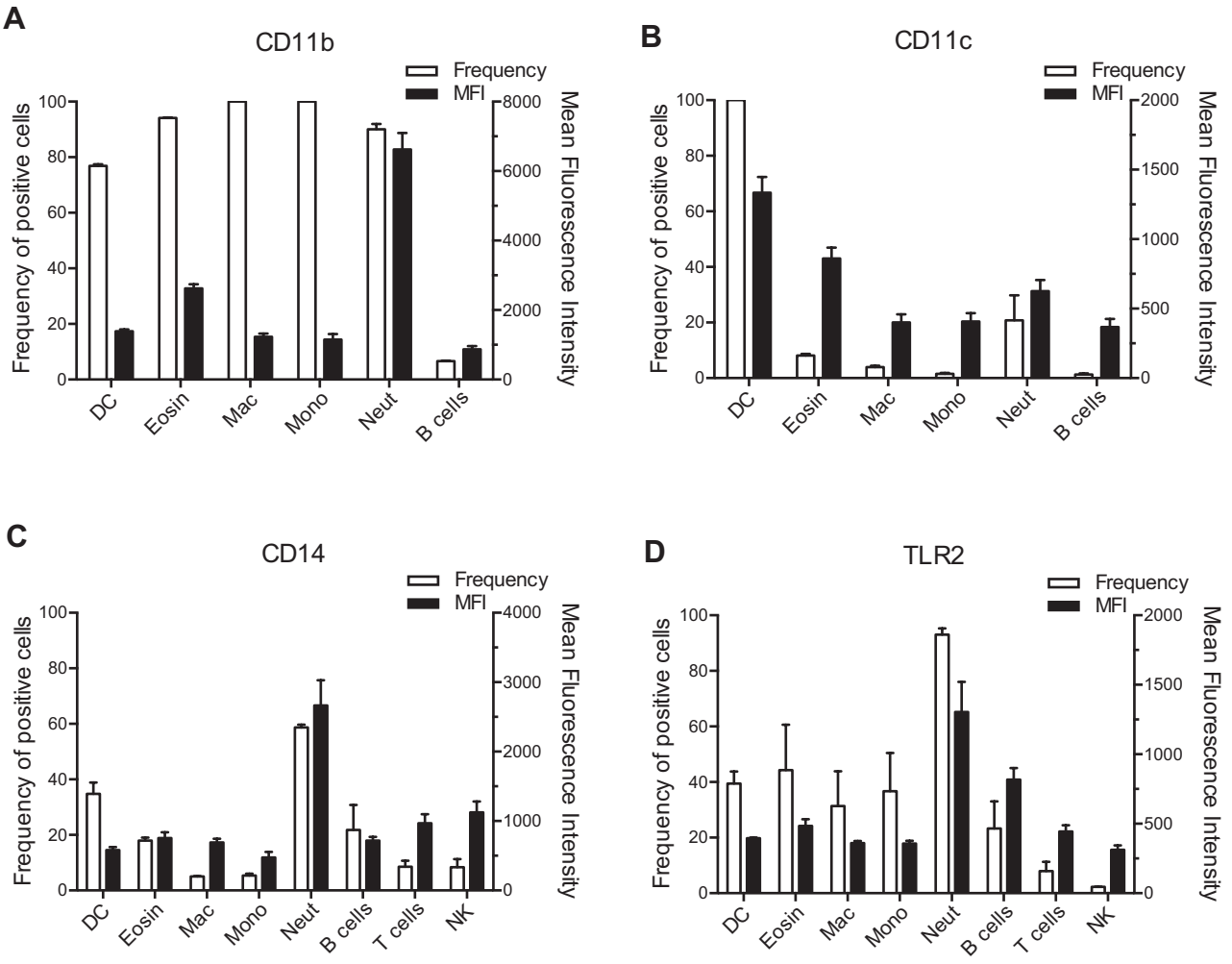

Fig. 6. Potential receptors are enriched on neutrophils. Splenocytes were suspended in RPMI containing FBS and NMS and stained with antibodies to identify cell types and fluorescently labeled (A) anti-CD11b, (B) anti-CD11c, (C) anti-CD14 or (D) anti-TLR2 was added to quantify expression of receptors on each cell type. The percentage of each cell type positive for the indicated marker is shown on the left *Y*-axis. The MFI for those cells positive for each marker is shown on the right *Y*-axis. DC, dendritic cells; Mac, macrophages; Mono, monocytes; Neut, neutrophils; Eosin, eosinophils; CD4, T helper cells; CD8, T cytotoxic cells; NK, NK cells.

splenocytes (Fig. 7A and B). Notably, non-preferred cell types did not become substitute targets for the T3SS when the normal targets (neutrophils) were neutralized via the antibody cocktail. We interpret these results to mean that the adhesin-independent targeting of neutrophils is specific and is mediated by at least one of the receptors blocked by the antibody cocktail.

We then assessed the ability of individual antibodies to block neutrophil targeting. We found that anti-CD14 treatment yielded only slight effects on targeting by either WT or the adhesin mutant (Fig. 8). In striking contrast, anti-CD11b severely reduced monocyte and neutrophil targeting (Fig. 8), similar to the blockade observed with the antibody cocktail (Fig. 7). Thus, it appears that CR3 is a major mediator of target cell specificity during plague infection.

Discussion

The tropism of *Yersinia* spp. for lymphoid tissue is well established, and recent work describing the targeting of innate immune cell populations for Yop injection during infection provides a satisfying correlation to tropism (Marketon *et al.*, 2005; Koberle *et al.*, 2009; Durand *et al.*, 2010). The professional phagocytes of the myeloid lineage are shared targets across the *Yersinia* spp., and

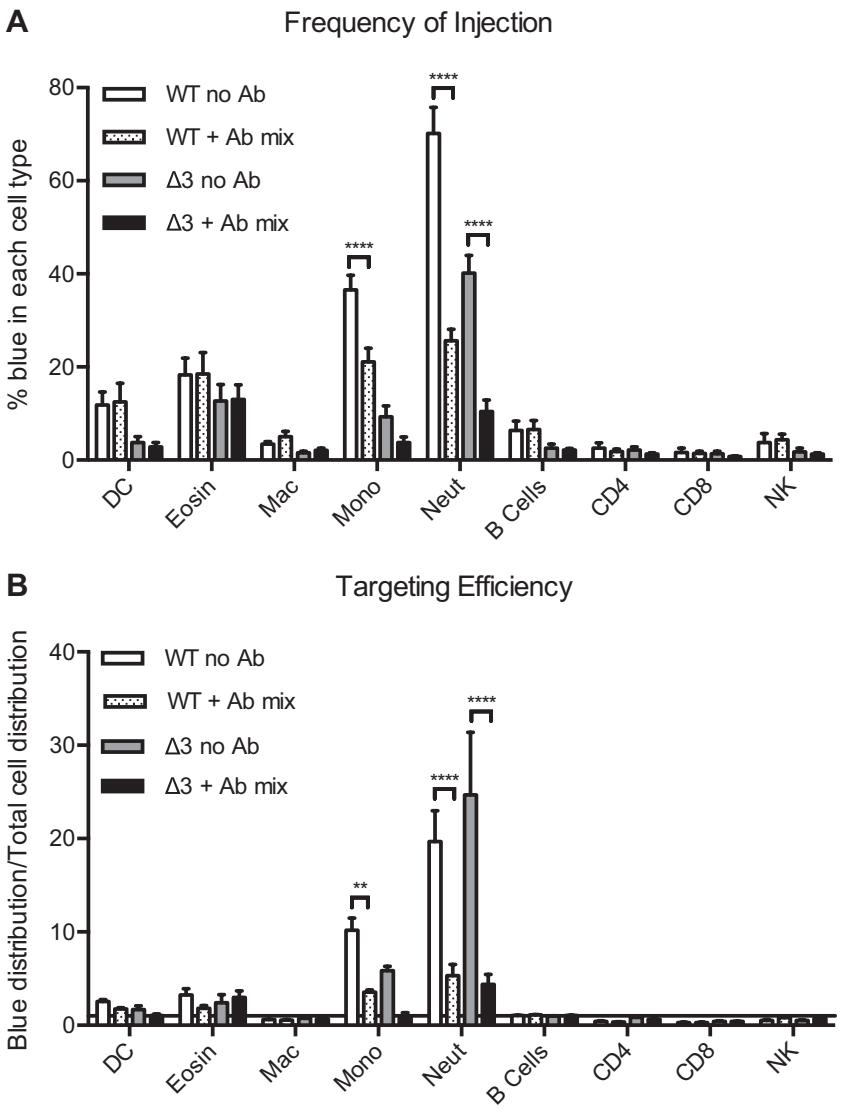

Fig. 7. Host receptors mediate target cell specificity. Splenocytes were left untreated (no Ab) or incubated with antibodies against CD14, CD11b and CD11c (+ Ab mix) prior to infecting with either WT or the Δ*ail/pla/psaA* mutant (Δ3) expressing YopM-Bla or Gst-Bla (not shown). Infections were performed in RPMI containing FBS, cytochalasin D and NMS. Cells were stained with CCF2-AM and antibodies, and then analysed by flow cytometry.
A. The percentage of blue cells for individual cell types is shown.
B. The targeting efficiency for each cell type is shown. Horizontal line at $Y = 1$ indicates no cell preference.
Two-way ANOVA with Bonferroni multiple comparisons test to determine significant differences for each cell type (**$P < 0.01$, ****$P < 0.0001$). DC, dendritic cells; Mac, macrophages; Mono, monocytes; Neut, neutrophils; Eosin, eosinophils; CD4, T helper cells; CD8, T cytotoxic cells; NK, NK cells.

this has been observed in lungs as well as spleens (Pechous *et al*., 2013; Paczosa *et al*., 2014). Of the myeloid cells, it seems that neutrophils are a particularly important target for the T3SS, since a failure to inactivate these potent mediators of inflammation compromises virulence, and correspondingly depletion of neutrophils can rescue virulence defects or alter the course of disease (Echeverry *et al*., 2007; Ye *et al*., 2009; 2011; Laws *et al*., 2010; Thorslund *et al*., 2013). Moreover, targeting of neutrophils is steadfast, and even when neutrophils are removed target cell specificity is not altered dramatically (Durand *et al*., 2010; Pechous *et al*., 2013; Paczosa *et al*., 2014). Given the conserved preference of neutrophil targeting across the *Yersinia* spp., how then is specificity mediated? Since receptor–ligand interactions had been demonstrated for *Yersinia* interactions with cultured cell lines (Kapperud *et al*., 1987; Isberg and Leong, 1990; Kienle *et al*., 1992; Young *et al*., 1992; Payne *et al*., 1998; Dersch and Isberg, 1999; Isberg *et al*., 2000; Lahteenmaki *et al*., 2001; Wiedemann *et al*., 2001; Eitel and Dersch, 2002; Lobo, 2006; Tsang *et al*., 2010; Yamashita *et al*., 2011), initial forays were focused logically on bacterial adhesins. However, the repertoire and functionality of adhesins is not conserved between *Yersinia*, and it remained to be determined if the same receptor–ligand interactions observed in cell culture infections contribute to specific targeting of primary immune cells *in vivo*. Indeed, the recent work on *Y. pseudotuberculosis* has begun to unravel the mystery of target cell selection by showing that bacterial adhesins only partially contribute to the process, while also revealing the additional complexities that host factors bring to the picture (Durand *et al*., 2010; Maldonado-Arocho *et al*., 2013; Paczosa *et al*., 2014).

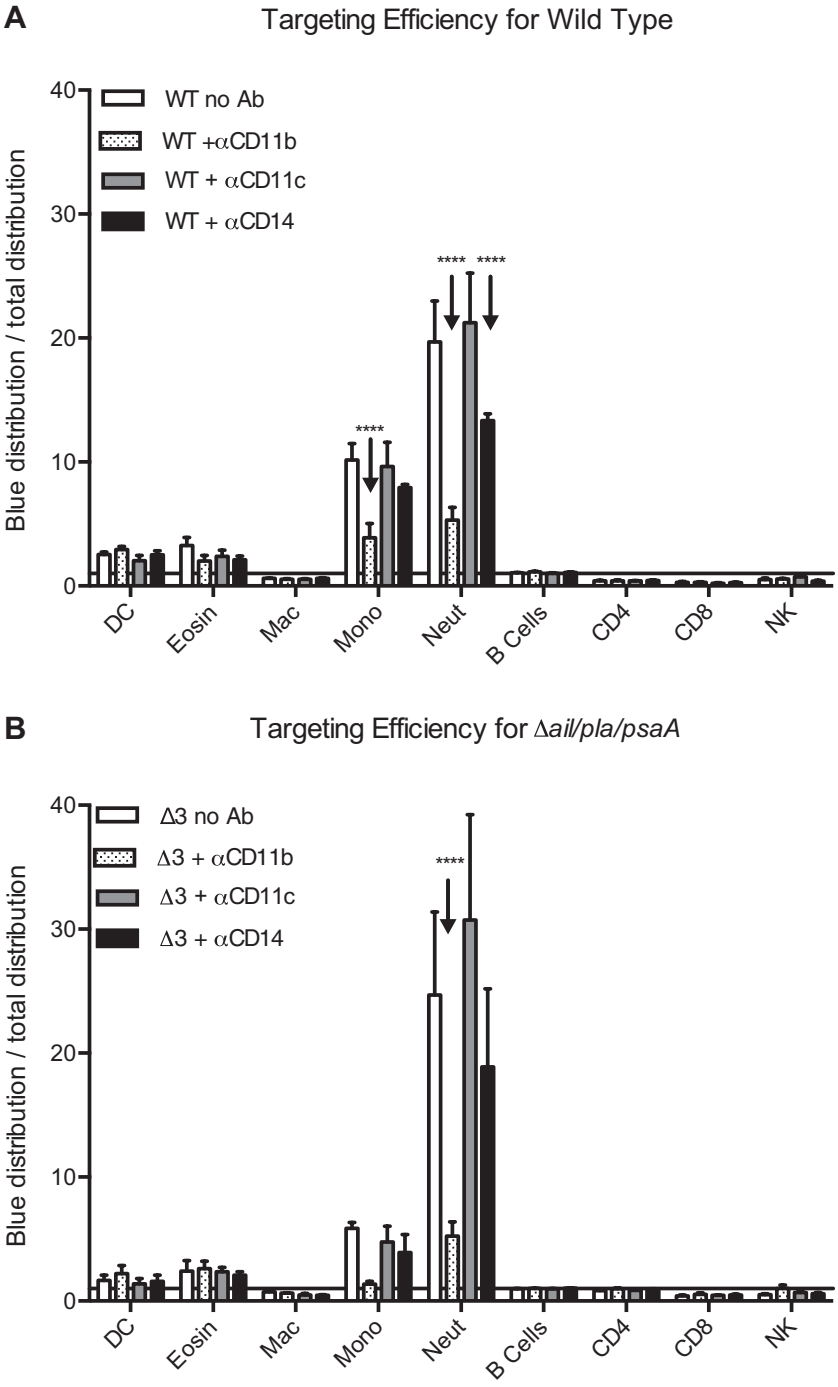

Fig. 8. CR3 is the primary mediator of neutrophil specificity. Splenocytes were left untreated (no Ab) or incubated with individual antibodies against CD14, CD11b or CD11c prior to infecting with either WT or the Δ*ail/pla/psaA* mutant ('Δ3') expressing YopM-Bla or Gst-Bla (not shown). Infections were performed in RPMI containing FBS, cytochalasin D and NMS. Cells were stained with CCF2-AM and antibodies, and then analysed by flow cytometry.
A. The targeting efficiency for each cell type infected with WT is shown.
B. The targeting efficiency for each cell type infected with the Δ*ail/pla/psaA* mutant is shown. Horizontal lines at $Y = 1$ indicate no cell preference.
Data were analysed using two-way ANOVA with Bonferroni multiple comparisons test (****$P < 0.0001$).

Using an attenuated strain in a mouse model of septicemic plague, it was demonstrated that *Y. pestis* targets several phagocytic, myeloid cell types (neutrophils, macrophages and dendritic cells) in the spleens of infected mice (Marketon *et al.*, 2005). This general target cell preference is maintained in lung tissue using a fully virulent strain in a pneumonic plague model (Pechous *et al.*, 2013). Interestingly, the dominant target population in lungs during the first few hours of infection was alveolar macrophages, but by 12 h post-infection, the targeting preference clearly transitioned over to neutrophils. A similar trend was observed during *Y. pseudotuberculosis* infection of lungs, and Ail and YadA were shown to mediate neutrophil targeting in that model (Paczosa *et al.*, 2014). Furthermore, *Y. pseudotuberculosis* Ail, YadA and invasin contribute to target cell selection

in spleens (Maldonado-Arocho *et al*., 2013). Though the factors mediating *in vivo* target cell specificity had not been characterized for *Y. pestis* yet, prior work demonstrated that Ail was the major adhesin required for T3SS-mediated delivery of Yop effectors into culture cell lines (Felek and Krukonis, 2009; Felek *et al*., 2010). Moreover, the Δ*ail* mutant was extremely attenuated in the septicemic plague model (Felek and Krukonis, 2009). We therefore set out to determine if Ail (or the other major adhesins) played a role in immune cell targeting.

We were surprised to find that the Δ*ail* mutant was capable of injecting Yops into host cells *in vivo* (Fig. 1). In fact, when spleens containing similar bacterial loads were compared, the total number of injected splenocytes did not differ between WT and the Δ*ail* mutant. However, further investigation revealed that the ability of the mutant to specifically target neutrophils for Yop injection *in vivo* was dramatically reduced (Fig. 4). Prior work already showed that Ail is required for resistance to complement-mediated killing and that Ail somehow inhibits a pro-inflammatory response to infection (Bartra *et al*., 2008; Felek and Krukonis, 2009; Hinnebusch *et al*., 2011; Ho *et al*., 2014). Since mouse serum is not bactericidal, and since an *ail* mutant is more attenuated in rats than in mice (Bartra *et al*., 2008; Kolodziejek *et al*., 2010; Hinnebusch *et al*., 2011), Ail likely has additional functions beyond preventing bacterial lysis because of membrane attack complex formation. Our data add to those observations regarding Ail's role as a virulence factor by demonstrating its requirement for proper target cell selection *in vivo*.

To explore the nature of the targeting defect for the Δ*ail* mutant, we developed an *ex vivo* assay to measure target cell selection. As was shown for the enteric *Yersinia* (Koberle *et al*., 2009; Durand *et al*., 2010), *Y. pestis* preference for innate immune cells was observed in the *ex vivo* assay (Fig. 5). Interestingly, B-cells were also targets of the T3SS; however, this observation was only true in the absence of mouse serum (Fig. 5A and B). When considered with the *in vivo* data (Marketon *et al*., 2005; Fig. 2), the results indicate that B-cells are not preferred targets for Yop injection in spleens of *Y. pestis* infected mice. That B- and T-cells are not preferred is not due to a lack of bacterial interaction. In fact bacteria interacted with these lymphocytes as well as myeloid populations, such as dendritic cells and macrophages (Supporting Information Fig. S7). It could be that some adhesion events do not bring the bacteria in direct contact with the cell surface, or it is possible that either the nature of the interaction or the quantity of interactions along an interface influence whether adhesion leads to injection. Regardless, the observations that myeloid cells, particularly neutrophils, are selected as preferred targets for Yop injection appears to be a general phenomenon, as it applies to targeting in lungs as well as spleen, and it is true for both *Y. pestis* and *Y. pseudotuberculosis* (Pechous *et al*., 2013; Paczosa *et al*., 2014).

During the course of our investigation into the role of bacterial adhesins during target cell selection, we were surprised to find no dramatic phenotype associated with any of the adhesin mutants during splenocyte infection in the absence of NMS (Fig. 5A and B and Supporting Information Fig. S5). This is in contrast to observations from infections of a variety of cultured cell lines (Felek and Krukonis, 2009; Felek *et al*., 2010). However, a role for Ail as a major adhesin was revealed once NMS was added to the *ex vivo* assays (Fig. 5E and F and Supporting Information Fig. S5C and D). Given that neutrophils were still preferentially targeted amidst overall reduced injection levels, and that the Δ*ail* and Δ*ail/pla/psaA* mutants behaved similarly, we conclude that target cell selection in the spleen is a combination of adhesin-dependent and -independent processes. The idea that adhesins serve a general role as facilitators of efficient host interaction is in agreement with *Y. pseudotuberculosis* observations, whereby adhesin mutants still demonstrated cell preference during splenocyte infection (Durand *et al*., 2010). In contrast, the preference for neutrophils in lung tissue was dependent upon the presence of either Ail or YadA during *Y. pseudotuberculosis* pneumonia (Paczosa *et al*., 2014). The role of *Y. pestis* adhesins in neutrophil targeting during pneumonic plague has not been addressed, but these data suggest that the use of adhesins during *Yersinia* infections may differ depending on the locale.

The observation that the *Y. pestis* Δ*ail* phenotype was only observed upon addition of NMS to splenocyte infections suggested a serum factor mediates Ail binding to host cells. This dependence on NMS for adhesin activity in *Y. pestis* is a notable point of difference compared with *Y. pseudotuberculosis*, whose adhesins do mediate host interactions even in serum-free medium (Maldonado-Arocho *et al*., 2013). Nonetheless, serum factors such as complement clearly impact the adhesin-dependent colonization of spleens during *Y. pseudotuberculosis* infection (Paczosa *et al*., 2014). Thus, while targeting in the lung may rely primarily on adhesins, targeting in the spleen may arise from a combination of adhesin and serum-dependent interactions.

Understanding the role of any potential serum factor in *Y. pestis* adhesin-dependent events is complicated by the observations that one or more heat-labile components of NMS reduced overall injection levels while also increasing the targeting efficiency for neutrophils (Fig. 5D and F), suggesting that there are likely multiple host factors acting in different ways. Since our assays already contained heat-inactivated FBS (fetal bovine serum) in the cell culture medium, existing heat-stabile components could

potentially mediate the general targeting of myeloid cells and B-cells in an adhesin-independent manner. Addition of NMS to the mixture would then contribute heat-labile factors to enhance neutrophil targeting.

One factor that is at least partially retained in heat-inactivated FBS is LBP (Meszaros *et al*., 1995). Lipopolysaccharide-binding protein binds to either free LPS or to bacterial surfaces and catalyses an interaction with CD14 and TLR4 (Wright *et al*., 1989; 1990; Kitchens, 2000; da Silva Correia *et al*., 2001). Notably, TLR4 is highly expressed by mouse myeloid cells and B-cells, but not T-cells (Applequist *et al*., 2002), supporting the idea that TLR4 may participate in an adhesin-independent interaction with *Y. pestis* and may lead to the broad targeting of B-cells and myeloid cells. CD14 is present as both a membrane receptor and as a soluble serum component, though it is heat-labile (Landmann *et al*., 1996a,b). Considering our data that show membrane CD14 is not present on the majority of murine splenic B-cells (Fig. 6), along with the fact that plasma from normal healthy mice does not contain high levels of soluble CD14 (Fearns *et al*., 1995), we would predict that the *Y. pestis*-TLR4 interaction on B-cells is direct, rather than facilitated by a CD14 intermediate. That type of interaction potentially could be outcompeted by myeloid cells, such as monocytes and neutrophils that have better expression of CD14 (Fig. 6). Furthermore, addition of NMS would provide an abundance of fresh LBP that could coat the bacteria and potentially obscure direct LPS-TLR4 binding, thereby suppressing Yop injection into B-cells. It is interesting to note that TLR4 knockout mice infected with *Y. pestis* show a faster time to death (Hajjar *et al*., 2012). That observation, as well as our data, suggests the possibility that in the absence of TLR4, there is less B-cell injection and instead the targeting of neutrophils is enhanced.

The serum factor(s) that mediate *Y. pestis* adhesin-dependent interactions and neutrophil targeting are heat-labile, and therefore, we considered complement proteins as candidates. The complement cascade can be initiated via three pathways: classical, MB-lectin and alternative, all of which culminate in the deposition of the opsonin C3b on the pathogen surface followed by formation of membrane attack complexes as well as binding to complement receptors (Walport, 2001). However, many pathogens circumvent this process by recruiting regulators or inactivators of complement proteins to the bacterial surface (Lambris *et al*., 2008). Importantly, Ail from *Y. pseudotuberculosis* and *Y. pestis* are nearly identical [only differing by up to two amino acids depending on the strain (Ho *et al*., 2012a; Kolodziejek *et al*., 2012; Tsang *et al*., 2013)] and both bind C4BP, which recruits Factor I to inactivate C4 to C4b (Ho *et al*., 2012a; 2014). Furthermore, *Y. pseudotuberculosis* Ail (and possibly *Y. pestis* Ail) binds to Factor H, which is a cofactor for Factor I and facilitates degradation of C3b to iC3b (Ho *et al*., 2012b; 2014). Additionally, *Y. pestis* Ail binds to C4, C4b and C3b (Ho *et al*., 2014). Therefore, it is possible that in the presence of NMS, *Y. pestis* becomes coated with ligands for complement receptors that contribute to target cell preference. When Ail is present, deposition of iC3b may predominate and direct the targeting of neutrophils via CR3.

In vivo, bacterial infection leads to high amounts of circulating opsonins (LBP, CD14 and complement proteins), which we hypothesize are likely contributors to efficient neutrophil targeting during *Y. pestis* infection. In the absence of Ail, interactions with cell types other than neutrophils dominate (Figs 3 and 4). This may be the result of the inability to bind iC3b directly (via Ail) or indirectly (via Ail-mediated recruitment of Factor I and Factor H; Ho *et al*., 2014). However, LBP and CD14 interactions would be unaffected, which might allow interactions with TLRs to prevail. In contrast to *in vivo* experiments (Fig. 4B), the *ex vivo* experiments (Fig. 5F) reveal a different trend for the *ail* mutant. Whereas the mutant was deficient for neutrophil targeting compared with WT *in vivo*, it was better than WT at targeting neutrophils *ex vivo*. There are a number of possible explanations for this difference. Firstly, the activation state of cells may differ and thereby affect expression of TLRs and CRs and subsequently the interactions with *Y. pestis*. Secondly, we expect that the potential opsonins would effectively be in unlimited supply during *in vivo* infections, since they are constantly being produced and production would likely be increased during infection. In contrast, serum used in *ex vivo* infections comes from naive mice and would not contain large amounts of C3 or CD14 (Triglia and Linscott, 1980; Fearns *et al*., 1995). Therefore, Ail may effectively capture the existing components to present iC3b as a CR3 ligand, but those components would be in limiting supply, and the Ail-mediated sequestration of iC3b and its regulators may result in further processing to yield C3dg or other inactive products. Additionally, the opposing Pla activity (Fig. 5D and Supporting Information Fig. S6) may arise from Pla-mediated degradation of these limited complement components into inactive fragments (Sodeinde *et al*., 1992). In the absence of Pla, it may be that Ail levels and/or activity may be higher, leading to increased Factor I recruitment and subsequent degradation of iC3b into C3dg, which is recognized by CR2 on B-cells (Weis *et al*., 1984), or into fragments that are not recognized by complement receptors. In contrast, when Ail is absent, spontaneous generation of C3b via the alternative pathway from the low levels of C3 in naive serum will provide limited deposition of C3b and this may be further degraded

into small amounts of iC3b by Pla. However, while Pla has been reported to degrade C3 (Sodeinde *et al*., 1992), it is not known whether Pla interacts with fluid-phase C3 products vs. those that have been deposited on the bacterial surface. It also is not known whether Pla degradation of C3 leads to products that can interact with CRs.

CR3 is the main receptor for iC3b (Ross and Lambris, 1982; Wright and Jong, 1986). Furthermore, there is evidence that CR3 binding is enhanced by concerted interactions with CD14/TLR2 (Troelstra *et al*., 1999; Sendide *et al*., 2005). Since CR3 is highly expressed by neutrophils, along with CD14 and TLR2 (Supporting Information Fig. S6; Sengelov, 1995), these proteins have the potential to be clustered in micro-domains on neutrophils. Interestingly, CD14 knockout mice show partial protection from plague infection, in terms of bacterial burden as well as percent survival (Depaolo *et al*., 2008), and this may reflect a supportive role for CD14 in enhancing neutrophil targeting *in vivo*. Future investigations will need to examine directly the roles of putative opsonins (C3/iC3b, LBP, soluble CD14) and their receptors during plague infection in order to determine the exact nature of the receptor–ligand interactions and their contributions towards target cell selection.

Experimental procedures

Bacterial strains and media

Yersinia pestis KIM D27, an attenuated variant of the *Y. pestis* mediaevalis strain KIM lacking the 102-kb *pgm* locus (Brubaker, 1969), was used as the parent strain. *Y. pestis* CHI30 (*yscU*::Mu) was generated by random mutagenesis of KIM D27 using *MuAphP1* (Marketon *et al*., 2005; Houppert *et al*., 2012). The streptomycin-resistant adhesin mutant Δ*ail* (KIM5-3001 Δ*ail*) has been described (Felek *et al*., 2010) and was used for mouse infections. Unmarked adhesin mutants (Δ*ail*, Δ*pla*Δ*psaA* and Δ*ail*Δ*pla*Δ*psaA*) in *Y. pestis* strain KIM D27 were constructed as described previously for KIM5-3001 using lambda-RED recombineering (Felek *et al*., 2010). The Bla reporter plasmids pMM83 (YopM-Bla) and pMM91 (Gst-Bla) have been described and were introduced into all *Y. pestis* strains to measure T3SS activity (Marketon *et al*., 2005). *Y. pestis* strains were propagated on Heart Infusion Agar (HIA) plates at 26°C for 2 days. Overnight cultures were grown in Heart Infusion Broth at 26°C. Antibiotics were added as appropriate to a final concentration of 20 μg ml^{-1} chloramphenicol and 50 μg ml^{-1} ampicillin.

Ethics statement

This study was carried out in accordance with the recommendations in the Guide for the Care and Use of Laboratory Animals of the National Institutes of Health. The work was approved by the Institutional Animal Care and Use Committee at Indiana University. Our approved protocol number is 12-051. All efforts were made to minimize suffering of the mice.

In vivo *infections*

Y. pestis overnight cultures were washed and diluted to appropriate densities in phosphate buffered saline (PBS). Female 6–7-week-old C57BL/6 mice (Harlan Laboratories, Indianapolis, IN, USA) were anaesthetized with isoflurane and retro-orbitally injected with 10^4 CFU of *Y. pestis* KIM5 carrying pMM83 (YopM-Bla) or pMM91 (GST-Bla), 10^6 CFU of *Y. pestis yscU*$^-$ (pMM83), or 10^6 CFU of Δ*ail* carrying pMM83 or pMM91. These doses were chosen based on preliminary experiments that monitored bacterial colonization resulting from a range of doses. We chose doses that were sufficient to ensure 100% of mice were colonized and would yield similar ranges of bacterial loads for KIM5 and the Δ*ail* mutant without causing mortality within the 3 day time frame. At daily intervals, mice were euthanized via CO_2 inhalation followed by cervical dislocation. Mice were perfused with 30 ml of sterile 1X PBS, and spleens were harvested and homogenized. A portion of the homogenate was serially diluted into PBS and plated onto HIA to enumerate the bacterial load. To assess injection of the Bla reporter, the remainder of the spleen suspension was processed for flow cytometry as follows. Cells were strained through a 70 μm nylon filter. Red blood cells were lysed with red blood cell lysis buffer (0.13 mM NH_4Cl, 0.017 mM Tris, 500 ml H_2O pH 7.2) for 5 min at room temperature. Splenocytes were pelleted at 1500× g for 3 min and resuspended in RPMI-1640 (Cellgro 10-040-CV) + 10% FBS. Cells were then stained with CCF2-AM (Invitrogen) at 0.2X for 1 h at room temperature. Cells were pelleted at 1500× g for 3 min and the supernatant was removed. Cells were then incubated with Fc Block (eBiosciences, Clone: 93) for 25 min on ice and then pelleted at 1500× g for 3 min. Splenocytes were then stained for 35 min on ice using the lymphoid and myeloid antibody panels described below. Splenocytes were then centrifuged and resuspended in HBSS Flow (1X HBSS, 0.5 mM EDTA, 25 mM HEPES, 2% BSA, pH 7.4) with propidium iodide (PI) solution (BD Pharmingen 556463) at 0.01 μg ml^{-1}. Flow cytometry was performed on a BD AriaII or a BD LSRII flow cytometer in the Indiana University Flow Cytometry Core Facility (IU FCCF), and data were analysed using FlowJo (Tree Star, Inc.) and Prism 5 (GraphPad Software, Inc.). The data are a compilation of three independent trials for WT infections ($n = 18$), two independent trials for Δ*ail* infections ($n = 11$) and one trial for *yscU*$^-$ infections ($n = 5$). The data are graphed showing mean and standard error with statistical analysis as indicated in figure legends.

Ex vivo *infections*

Ex vivo injection assays were performed as described by Houppert *et al*. (2013) with minor modifications indicated below. Briefly, spleens from naïve female 6–7-week-old C57BL/6 mice were homogenized in 1 ml of PBS. The homogenate was incubated for 5 min at room temperature with red blood cell lysis buffer, pelleted by centrifugation at 1500× g for 3 min, and resuspended in RPMI supplemented with 10% heat-inactivated FBS (HyClone) and strained through a 70 μm filter. Cells were incubated with 1 μg ml^{-1} cytochalasin D (Sigma) for 30 min prior to infection to inhibit phagocytosis. Mid-exponential-phase *Y. pestis* cultures were incubated for 1.5 h at 37°C to induce the T3SS. 1×10^6 splenocytes were infected with indicated strains of *Y. pestis* carrying plasmids expressing YopM-Bla (or GST-Bla as a negative control) in 100 μl RPMI+FBS with or without

10% mouse serum (MP Biomedicals). Where indicated, heat-inactivated (56°C, 30 min) mouse serum was used. Bacteria were added to splenocytes at multiplicity of infection (MOI) of 1, and the infection mixture was centrifuged at 500× g for 5 min to facilitate cell contact. Infections were incubated at 37°C, 5% CO_2 for 1.5 h. Infected splenocytes were collected by centrifugation and resuspended in fresh medium supplemented with 50 μg ml^{-1} kanamycin to stop bacterial growth and injection. Cells were stained with 1X CCF2-AM for 1 h at room temperature. Cells were pelleted at 1500× g for 3 min, and resuspended in HBSS Flow. Next, the cells were incubated with Fc Block for 20 min on ice. Cells were pelleted at 1500× g for 3 min, resuspended in HBSS Flow. Splenocytes were then stained for 35 min on ice using the lymphoid and myeloid antibody panels described below. Following the staining, cells were pelleted and resuspended in HBSS Flow containing PI (0.075 μg ml^{-1}). Flow cytometry was performed on a BD LSRII flow cytometer in the IU FCCF, and data were analysed using FlowJo and GraphPad Prism. The data are graphed showing mean and standard error with statistical analysis as indicated in figure legends.

Identification of immune cell populations

To identify the major splenocyte immune cell populations, the cell suspensions were subjected to staining by the following two antibody cocktails.

Lymphoid panel. CD19-PeCy7 (BD Pharmingen; clone 1D3), CD4-APC-eFluor 780 (eBiosciences; clone RM4-5), CD8-PerCP-eFluor 710 (eBiosciences; clone 53-6.7) and NK1.1-APC (BD Pharmingen; clone PK136).

Myeloid panel. CD11b-PeCy7 (BD Pharmingen; clone 1D3), CD11c-APC (BD Pharmingen; clone HL3), major histocompatibility complex class II (MHC-II)-PerCP-eFluor 710 (eBiosciences; clone M5/114.15.2) and GR-1-APC-Cy7 (BD Pharmingen; clone RB6-8C5).

The flow cytometry gating strategy is described in Supporting Information Fig. S2 and is based on previous work (Geddes *et al.*, 2007; Rose *et al.*, 2012). Forward and side scatter were used to separate and discard debris and doublets. Live cells were identified by PI exclusion and forward scatter. Live events were then gated to identify B-cells (CD4$^-$ CD8$^-$ CD19$^+$ NK1.1$^-$), T helper cells (CD4$^+$ CD8$^-$), T cytotoxic cells (CD4$^-$ CD8$^+$), NK cells (CD4$^-$ CD8$^-$ CD19$^-$ NK1.1$^+$), neutrophils (SSC^{Int} GR1^{Hi}), eosinophils (SSC$^{Hi/Int}$ GR1^{Int}), dendritic cells (CD11c$^+$), macrophages (MHC-II$^-$ CD11c$^-$ CD11b$^+$ GR1$^-$) and monocytes (MHC-II$^-$ CD11c$^-$ CD11b$^+$ GR1^{Int}). The percentage of blue (injected) cells was determined for the total population and for each individual cell type cells (termed 'frequency of injection' for each cell type). The distribution of all cell types was also determined, as well as the distribution of cell types within the blue (injected) population. To calculate the 'targeting efficiency', the relative proportion of a cell type in the blue population was divided by the relative proportion of the cell type in the total splenocyte population (distribution in blue cells/distribution in total cells) as described in Supporting Information Fig. S5.

Surface marker profiles

Spleens from naïve 6–7-week-old female mice were harvested and processed as described above for *ex vivo* infections. Cells were incubated with 1 μg ml^{-1} cytochalasin D (Sigma) for 1.5 h at 37°C, 5% CO_2 to be consistent with our infection conditions. The splenocytes were pelleted by centrifugation at 1500× g for 3 min, resuspended in HBSS Flow and incubated with Fc Block for 20 min on ice. Then, the cells were pelleted at 1500× g for 3 min and resuspended in HBSS Flow containing the relevant antibody cocktail. Two different antibody panels were used to test the prevalence and intensity of CD14 and TLR2 markers on myeloid cells.

Myeloid TLR2 panel. TLR2-PeCy7 (eBiosciences; clone: T2.5), CD11b-PeCy5 (eBiosciences; clone: M1/70), CD11c-AlexaFluor 700 (eBiosciences; clone: N418), GR-1-PeCy5.5 (eBiosciences; clone: RB6-8C5), MHC-II-APC-eFluor 780 (eBiosciences; clone: M5/114.15.12).

Myeloid CD14 panel. A similar panel was used with CD14-APC (eBiosciences; clone: Sa2-8) and CD11b-PeCy7 (BD Pharmingen; clone: M1/70) replacing TLR2-PeCy7 and CD11b-PeCy5.

Lymphoid panels. For investigation of the lymphoid cells, three panels of three antibodies were used: [Lymphoid panel 1] CD19-AlexaFluor 700 (BD Pharmingen; clone: 1D3), TLR2-PeCy7 and CD14-APC; [Lymphoid panel 2] CD3-AlexaFluor 700 (BD Pharmingen; clone: 17A2), TLR2-PeCy7 and CD14-APC; and [Lymphoid panel 3] NK1.1-AF700 (BD Pharmingen; clone: PK136), TLR2-PeCy7 and CD14-APC.

Staining was done for 35 min on ice and then, the cells were pelleted at 1500× g for 3 min. Following staining, the cells were resuspended in HBSS Flow containing PI (0.075 μg ml^{-1}). The flow cytometry gating strategy outlined in Supporting Information Fig. S2 was used with the following modifications for identifying lymphoid cells. Live events were gated to identify B-cells positive for TLR2 or CD14 (CD19$^+$ TLR2$^+$) or (CD19$^+$ CD14$^+$) respectively. Similarly, T-cells (CD3$^+$ TLR2$^+$) or (CD3$^+$ CD14$^+$) and NK cells (NK1.1$^+$ TLR2$^+$) or (NK1.1$^+$ CD14$^+$) were gated to identify those positive for the surface markers. The percentage of TLR2 and CD14 was determined for each individual cell type along with the MFI of either TLR2 or CD14. In addition, the percentage of CD11b or CD11c was determined for each of the myeloid cell populations, as well as the corresponding MFIs. Mean fluorescence intensity was calculated by finding the mean intensity for TLR2+, CD14+, CD11b+ or CD11c+ cells within each population. Flow cytometry was performed on a BD LSRII and data was analysed using FlowJo and GraphPad Prism. The data are graphed showing mean and standard error. Statistical analysis was done using one-way analysis of variance (ANOVA) with Dunnett's multiple comparison test.

Serum depletion or blocking experiments

Ex vivo infections were performed as described above with the following exceptions.

Depletion of IgG. IgG was depleted from serum by incubating 0.5 ml Protein A/G Agarose (Pierce) with 1 ml of mouse serum at 4°C, overnight. The beads were centrifuged and serum was removed and stored on ice until used.

Receptor blocking. For blocking surface receptors on splenocytes, cells were incubated with FcBlock for 20 min at 37°C and then with the following antibodies (1:50 dilution) for 35 min at 37°C prior to infection: anti-CD21/35 (Biolegend, clone 7E9), anti-CD11b (same as above), anti-CD11c (same as above), anti-CD14 (Biolegend, clone Sa-14-2). After incubation with antibodies, infections were carried out according to our *ex vivo* protocol.

Fibronectin receptor blocking. In a separate blocking experiment, cells were pretreated with anti-fibronectin (Sigma, F3648) prior to infection.

Adhesion assays

The indicated *Y. pestis* strains were transformed with pGFPuv (Clontech), so the strains constitutively expressed a GFP variant that can be excited with UV or violet light. To detect bacterial adhesion to specific cell types, *ex vivo* infection assays were performed as described above using *Y. pestis* strains expressing GFPuv. Flow cytometry was performed using the BD LSRII cytometer. GFPuv fluorescence was detected from the violet laser using a FITC detector and the immunophenotyping panel was the same as described above for *ex vivo* assays. Data shown represent means with standard deviation. Statistical analysis was done using one-way ANOVA with Tukey post-hoc test.

Acknowledgements

We would like to thank Dr. William DePaolo for many helpful discussions and technical advice, Dr. Joan Mecsas for helpful discussions and critical insight and Christiane Hassel in the IU Flow Cytometry Core Facility for technical training and guidance. E.S.K. acknowledges support from NIH/NIAID grants R03 AI092318 and R21 AI090194. M.M.M acknowledges support through startup funds from Indiana University-Bloomington, from the Office of the Vice Provost of Research at IU-B through the Faculty Research Support Program, and from NIH/NIAID grant R01 AI07055, as well as membership within and support from the Region V 'Great Lakes' Regional Center of Excellence in Biodefense and Emerging Infectious Diseases Consortium (NIH Award 1-U54-AI-057153).

References

Abramov, V.M., Khlebnikov, V.S., Vasiliev, A.M., Kosarev, I.V., Vasilenko, R.N., Kulikova, N.L., *et al*. (2007) Attachment of LcrV from *Yersinia pestis* at dual binding sites to human TLR-2 and human IFN-gamma receptor. *J Proteome Res* **6:** 2222–2231.

Applequist, S.E., Wallin, R.P., and Ljunggren, H.G. (2002) Variable expression of Toll-like receptor in murine innate and adaptive immune cell lines. *Int Immunol* **14:** 1065–1074.

Bartra, S.S., Styer, K.L., O'Bryant, D.M., Nilles, M.L., Hinnebusch, B.J., Aballay, A., and Plano, G.V. (2008) Resistance of *Yersinia pestis* to complement-dependent killing is mediated by the Ail outer membrane protein. *Infect Immun* **76:** 612–622.

Ben-Efraim, S., Aronson, M., and Bichowsky-Slomnicki, L. (1961) New antigenic component of *Pasteurella pestis* formed under specific conditions of pH and temperature. *J Bacteriol* **81:** 704–714.

Biedzka-Sarek, M., Venho, R., and Skurnik, M. (2005) Role of YadA, Ail, and lipopolysaccharide in serum resistance of *Yersinia enterocolitica* Serotype O:3. *Infect Immun* **73:** 2232–2244.

Bliska, J.B., Copass, M.C., and Falkow, S. (1993) The *Yersinia pseudotuberculosis* adhesin YadA mediates intimate bacterial attachment to and entry into HEp-2 cells. *Infect Immun* **61:** 3914–3921.

Blom, A.M., Kask, L., and Dahlback, B. (2003) CCP1-4 of the C4b-binding protein alpha-chain are required for factor I mediated cleavage of complement factor C3b. *Mol Immunol* **39:** 547–556.

Brubaker, R.R. (1969) Mutation rate to non-pigmentation in *Pasteurella pestis*. *J Bacteriol* **98:** 1404–1406.

Buttner, D. (2012) Protein export according to schedule: architecture, assembly, and regulation of type III secretion systems from plant- and animal-pathogenic bacteria. *Microbiol Mol Biol Rev* **76:** 262–310.

Charpentier, X., and Oswald, E. (2004) Identification of the secretion and translocation domain of the enteropathogenic and enterohemorrhagic *Escherichia coli* effector Cif, using TEM-1 beta-lactamase as a new fluorescence-based reporter. *J Bacteriol* **186:** 5486–5495.

Depaolo, R.W., Tang, F., Kim, I., Han, M., Levin, N., Ciletti, N., *et al*. (2008) Toll-like receptor 6 drives differentiation of tolerogenic dendritic cells and contributes to LcrV-mediated plague pathogenesis. *Cell Host Microbe* **4:** 350–361.

Dersch, P., and Isberg, R.R. (1999) A region of the *Yersinia pseudotuberculosis* invasin protein enhances integrin-mediated uptake into mammalian cells and promotes self-association. *EMBO J* **18:** 1199–1213.

Dewoody, R.S., Merritt, P.M., and Marketon, M.M. (2013) Regulation of the *Yersinia* type III secretion system: traffic control. *Front Cell Infect Microbiol*. doi: 10.3389/fcimb.2013.00004.

Durand, E.A., Maldonado-Arocho, F.J., Castillo, C., Walsh, R.L., and Mecsas, J. (2010) The presence of professional phagocytes dictates the number of host cells targeted for Yop translocation during infection. *Cell Microbiol* **12:** 1064–1082.

Echeverry, A., Schesser, K., and Adkins, B. (2007) Murine neonates are highly resistant to *Yersinia enterocolitica* following orogastric exposure. *Infect Immun* **75:** 2234–2243.

Eitel, J., and Dersch, P. (2002) The YadA protein of *Yersinia pseudotuberculosis* mediates high-efficiency uptake into human cells under environmental conditions in which invasin is repressed. *Infect Immun* **70:** 4880–4891.

Fearns, C., Kravchenko, V.V., Ulevitch, R.J., and Loskutoff, D.J. (1995) Murine CD14 gene expression *in vivo*: extramyeloid synthesis and regulation by lipopolysaccharide. *J Exp Med* **181:** 857–866.

Felek, S., and Krukonis, E.S. (2009) The *Yersinia pestis* Ail protein mediates binding and Yop delivery to host cells required for plague virulence. *Infect Immun* **77:** 825–836.

Felek, S., Tsang, T.M., and Krukonis, E.S. (2010) Three *Yersinia pestis* adhesins facilitate Yop delivery to eukaryotic cells and contribute to plague virulence. *Infect Immun* **78:** 4134–4150.

Gage, K.L., and Kosoy, M.Y. (2005) Natural history of plague: perspectives from more than a century of research. *Annu Rev Entomol* **50:** 505–528.

Galindo, C.L., Rosenzweig, J.A., Kirtley, M.L., and Chopra, A.K. (2011) Pathogenesis of *Y. enterocolitica* and *Y. pseudotuberculosis* in human yersiniosis. *J Pathog* **2011:** 182051.

Geddes, K., Cruz, F., and Heffron, F. (2007) Analysis of cells targeted by *Salmonella* type III secretion *in vivo*. *PLoS Pathog* **3:** e196.

Grunwald, U., Fan, X., Jack, R.S., Workalemahu, G., Kallies, A., Stelter, F., and Schutt, C. (1996) Monocytes can phagocytose Gram-negative bacteria by a CD14-dependent mechanism. *J Immunol* **157:** 4119–4125.

Hajjar, A.M., Ernst, R.K., Fortuno, E.S., 3rd, Brasfield, A.S., Yam, C.S., Newlon, L.A., *et al*. (2012) Humanized TLR4/MD-2 mice reveal LPS recognition differentially impacts susceptibility to *Yersinia pestis* and *Salmonella enterica*. *PLoS Pathog* **8:** e1002963.

Handley, S.A., Newberry, R.D., and Miller, V.L. (2005) *Yersinia enterocolitica* invasin-dependent and invasin-independent mechanisms of systemic dissemination. *Infect Immun* **73:** 8453–8455.

Hinnebusch, B.J., Jarrett, C.O., Callison, J.A., Gardner, D., Buchanan, S.K., and Plano, G.V. (2011) Role of the *Yersinia pestis* Ail protein in preventing a protective polymorphonuclear leukocyte response during bubonic plague. *Infect Immun* **79:** 4984–4989.

Ho, D.K., Riva, R., Kirjavainen, V., Jarva, H., Ginstrom, E., Blom, A.M., *et al*. (2012a) Functional recruitment of the human complement inhibitor C4BP to *Yersinia pseudotuberculosis* outer membrane protein Ail. *J Immunol* **188:** 4450–4459.

Ho, D.K., Riva, R., Skurnik, M., and Meri, S. (2012b) The *Yersinia pseudotuberculosis* outer membrane protein Ail recruits the human complement regulatory protein factor H. *J Immunol* **189:** 3593–3599.

Ho, D.K., Skurnik, M., Blom, A.M., and Meri, S. (2014) *Yersinia pestis* Ail recruitment of C4b-binding protein leads to factor I-mediated inactivation of covalently and noncovalently bound C4b. *Eur J Immunol* **44:** 742–751.

Houppert, A.S., Kwiatkowski, E., Glass, E.M., DeBord, K.L., Merritt, P.M., Schneewind, O., and Marketon, M.M. (2012) Identification of chromosomal genes in *Yersinia pestis* that influence type III secretion and delivery of Yops into target cells. *PLoS ONE* **7:** e34039.

Houppert, A.S., Bohman, L., Merritt, P.M., Cole, C.B., Caulfield, A.J., Lathem, W.W., and Marketon, M.M. (2013) RfaL is required for *Yersinia pestis* type III secretion and virulence. *Infect Immun* **81:** 1186–1197.

Iriarte, M., Vanooteghem, J.C., Delor, I., Diaz, R., Knutton, S., and Cornelis, G.R. (1993) *The Myf fibrillae of Yersinia enterocolitica*. *Mol Microbiol* **9:** 507–520.

Isberg, R.R., and Leong, J.M. (1990) Multiple beta 1 chain integrins are receptors for invasin, a protein that promotes bacterial penetration into mammalian cells. *Cell* **60:** 861–871.

Isberg, R.R., Hamburger, Z., and Dersch, P. (2000) Signaling and invasin-promoted uptake via integrin receptors. *Microbes Infect* **2:** 793–801.

Kapperud, G., Namok, E., and Sarpeid, H.J. (1985) Temperature-inducible surface fibrillae associated with the virulence plasmid of *Yersinia enterocolitica* and *Yersinia pseudotuberculosis*. *Infect Immun* **47:** 561–566.

Kapperud, G., Namork, E., Skurnik, M., and Nesbakken, T. (1987) Plasmid-mediated surface fibrillae of *Yersinia pseudotuberculosis* and *Yersinia enterocolitica*: relationship to the outer membrane protein Yop1 and possible importance for pathogenesis. *Infect Immun* **55:** 2247–2254.

Kienle, Z., Emody, L., Svanborg, C., and O'Toole, P.W. (1992) Adhesive properties conferred by the plasminogen activator of *Yersinia pestis*. *J Gen Microbiol* **138** (Part 8)**:** 1679–1687.

Kitchens, R.L. (2000) Role of CD14 in cellular recognition of bacterial lipopolysaccharides. *Chem Immunol* **74:** 61–82.

Koberle, M., Klein-Gunther, A., Schutz, M., Fritz, M., Berchtold, S., Tolosa, E., *et al*. (2009) *Yersinia enterocolitica* targets cells of the innate and adaptive immune system by injection of Yops in a mouse infection model. *PLoS Pathog* **5:** e1000551.

Kolodziejek, A.M., Sinclair, D.J., Seo, K.S., Schnider, D.R., Deobald, C.F., Rohde, H.N., *et al*. (2007) Phenotypic characterization of OmpX, an Ail homologue of *Yersinia pestis* KIM. *Microbiology* **153:** 2941–2951.

Kolodziejek, A.M., Schnider, D.R., Rohde, H.N., Wojtowicz, A.J., Bohach, G.A., Minnich, S.A., and Hovde, C.J. (2010) Outer membrane protein X (Ail) contributes to *Yersinia pestis* virulence in pneumonic plague and its activity is dependent on the lipopolysaccharide core length. *Infect Immun* **78:** 5233–5243.

Kolodziejek, A.M., Hovde, C.J., and Minnich, S.A. (2012) *Yersinia pestis* Ail: multiple roles of a single protein. *Front Cell Infect Microbiol*. doi: 10.3389/fcimb.2012.00103.

Lahteenmaki, K., Kukkonen, M., and Korhonen, T.K. (2001) The Pla surface protease/adhesin of *Yersinia pestis* mediates bacterial invasion into human endothelial cells. *FEBS Lett* **504:** 69–72.

Lambris, J.D., Ricklin, D., and Geisbrecht, B.V. (2008) Complement evasion by human pathogens. *Nat Rev Microbiol* **6:** 132–142.

Landmann, R., Knopf, H.P., Link, S., Sansano, S., Schumann, R., and Zimmerli, W. (1996a) Human monocyte CD14 is upregulated by lipopolysaccharide. *Infect Immun* **64:** 1762–1769.

Landmann, R., Reber, A.M., Sansano, S., and Zimmerli, W. (1996b) Function of soluble CD14 in serum from patients with septic shock. *J Infect Dis* **173:** 661–668.

Laws, T.R., Davey, M.S., Titball, R.W., and Lukaszewski, R. (2010) Neutrophils are important in early control of lung infection by *Yersinia pestis*. *Microbes Infect* **12:** 331–335.

Leo, J.C., and Skurnik, M. (2011) Adhesins of human pathogens from the genus *Yersinia*. *Adv Exp Med Biol* **715:** 1–15.

Lobo, L.A. (2006) Adhesive properties of the purified plasminogen activator Pla of *Yersinia pestis*. *FEMS Microbiol Lett* **262:** 158–162.

Maldonado-Arocho, F.J., Green, C., Fisher, M.L., Paczosa, M.K., and Mecsas, J. (2013) Adhesins and host serum factors drive Yop translocation by *Yersinia* into professional phagocytes during animal infection. *PLoS Pathog* **9:** e1003415.

Marketon, M.M., DePaolo, R.W., DeBord, K.L., Jabri, B., and Schneewind, O. (2005) Plague bacteria target immune cells during infection. *Science* **309:** 1739–1741.

Marra, A., and Isberg, R.R. (1997) Invasin-dependent and invasin-independent pathways for translocation of *Yersinia pseudotuberculosis* across the Peyer's patch intestinal epithelium. *Infect Immun* **65:** 3412–3421.

Meszaros, K., Aberle, S., White, M., and Parent, J.B. (1995) Immunoreactivity and bioactivity of lipopolysaccharide-binding protein in normal and heat-inactivated sera. *Infect Immun* **63:** 363–365.

Miller, V.L., and Falkow, S. (1988) Evidence for two genetic loci in *Yersinia enterocolitica* that can promote invasion of epithelial cells. *Infect Immun* **56:** 1242–1248.

Paczosa, M.K., Fisher, M.L., Maldonado-Arocho, F.J., and Mecsas, J. (2014) *Yersinia pseudotuberculosis* uses Ail and YadA to circumvent neutrophils by directing Yop translocation during lung infection. *Cell Microbiol* **16:** 247–268.

Payne, D., Tatham, D., Williamson, E.D., and Titball, R.W. (1998) The pH 6 antigen of *Yersinia pestis* binds to beta1-linked galactosyl residues on glycosphingolipids. *Infect Immun* **66:** 4545–4548.

Pechous, R.D., Sivaraman, V., Price, P.A., Stasulli, N.M., and Goldman, W.E. (2013) Early host cell targets of *Yersinia pestis* during primary pneumonic plague. *PLoS Pathog* **9:** e1003679.

Pepe, J.C., Wachtel, M.R., Wagar, E., and Miller, V.L. (1995) Pathogenesis of defined invasion mutants of *Yersinia enterocolitica* in a BALB/c mouse model of infection. *Infect Immun* **63:** 4837–4848.

Perry, R.D., and Fetherston, J.D. (1997) *Yersinia pestis* – etiologic agent of plague. *Clin Microbiol Rev* **10:** 35–66.

Pieper, R., Huang, S.T., Clark, D.J., Robinson, J.M., Alami, H., Parmar, P.P., *et al*. (2009) Integral and peripheral association of proteins and protein complexes with *Yersinia pestis* inner and outer membranes. *Proteome Sci*. doi: 10.1186/1477-5956-7-5.

Pierson, D.E., and Falkow, S. (1993) The *ail* gene of *Yersinia enterocolitica* has a role in the ability of the organism to survive serum killing. *Infect Immun* **61:** 1846–1852.

Rose, S., Misharin, A., and Perlman, H. (2012) A novel Ly6C/Ly6G-based strategy to analyze the mouse splenic myeloid compartment. *Cytometry A* **81:** 343–350.

Ross, G.D., and Lambris, J.D. (1982) Identification of a C3bi-specific membrane complement receptor that is expressed on lymphocytes, monocytes, neutrophils, and erythrocytes. *J Exp Med* **155:** 96–110.

Ruckdeschel, K., Deuretzbacher, A., and Haase, R. (2008) Crosstalk of signalling processes of innate immunity with *Yersinia* Yop effector functions. *Immunobiology* **213:** 261–269.

Schindler, M.K., Schutz, M.S., Muhlenkamp, M.C., Rooijakkers, S.H., Hallstrom, T., Zipfel, P.F., and Autenrieth, I.B. (2012) *Yersinia enterocolitica* YadA mediates complement evasion by recruitment and inactivation of C3 products. *J Immunol* **189:** 4900–4908.

Sebbane, F., Gardner, D., Long, D., Gowen, B.B., and Hinnebusch, B.J. (2005) Kinetics of disease progression and host response in a rat model of bubonic plague. *Am J Pathol* **166:** 1427–1439.

Sendide, K., Reiner, N.E., Lee, J.S., Bourgoin, S., Talal, A., and Hmama, Z. (2005) Cross-talk between CD14 and complement receptor 3 promotes phagocytosis of Mycobacteria: regulation by phosphatidylinositol 3-kinase and cytohesin-1. *J Immunol* **174:** 4210–4219.

Sengelov, H. (1995) Complement receptors in neutrophils. *Crit Rev Immunol* **15:** 107–131.

da Silva Correia, J., Soldau, K., Christen, U., Tobias, P.S., and Ulevitch, R.J. (2001) Lipopolysaccharide is in close proximity to each of the proteins in its membrane receptor complex. transfer from CD14 to TLR4 and MD-2. *J Biol Chem* **276:** 21129–21135.

Sing, A., Rost, D., Tvardovaskaia, N., Roggenkamp, A., Wiedemann, A., Kirschning, C., *et al*. (2002) *Yersinia* V-antigen exploits Toll-like receptor 2 and CD14 for interleukin 10-mediated immunosuppression. *J Exp Med* **196:** 1017–1024.

Sodeinde, O.A., Sample, A.K., Brubaker, R.R., and Goguen, J.D. (1988) Plasminogen activator/coagulase gene of *Yersinia pestis* is responsible for degradation of plasmid-encoded outer membrane proteins. *Infect Immun* **56:** 2749–2752.

Sodeinde, O.A., Subrahmanyam, Y.V., Stark, K., Quan, T., Bao, Y., and Goguen, J.D. (1992) A surface protease and the invasive character of plague. *Science* **258:** 1004–1007.

Thorslund, S.E., Ermert, D., Fahlgren, A., Erttmann, S.F., Nilsson, K., Hosseinzadeh, A., *et al*. (2013) Role of YopK in *Yersinia pseudotuberculosis* resistance against polymorphonuclear leukocyte defense. *Infect Immun* **81:** 11–22.

Triglia, R.P., and Linscott, W.D. (1980) Titers of nine complement components, conglutinin and C3b-inactivator in adult and fetal bovine sera. *Mol Immunol* **17:** 741–748.

Troelstra, A., de Graaf-Miltenburg, L.A., van Bommel, T., Verhoef, J., Van Kessel, K.P., and Van Strijp, J.A. (1999) Lipopolysaccharide-coated erythrocytes activate human neutrophils via CD14 while subsequent binding is through CD11b/CD18. *J Immunol* **162:** 4220–4225.

Tsang, T.M., Felek, S., and Krukonis, E.S. (2010) Ail binding to fibronectin facilitates *Yersinia pestis* binding to host cells and Yop delivery. *Infect Immun* **78:** 3358–3368.

Tsang, T.M., Wiese, J.S., Felek, S., Kronshage, M., and Krukonis, E.S. (2013) Ail proteins of *Yersinia pestis* and *Y. pseudotuberculosis* have different cell binding and invasion activities. *PLoS ONE* **8:** e83621.

Uliczka, F., Pisano, F., Schaake, J., Stolz, T., Rohde, M., Fruth, A., *et al*. (2011) Unique cell adhesion and invasion properties of *Yersinia enterocolitica* O:3, the most frequent cause of human yersiniosis. *PLoS Pathog* **7:** e1002117.

Viboud, G.I., and Bliska, J.B. (2005) *Yersinia* outer proteins: role in modulation of host cell signaling responses and pathogenesis. *Annu Rev Microbiol* **59:** 69–89.

Walport, M.J. (2001) Complement. First of two parts. *N Engl J Med* **344:** 1058–1066.
Weis, J.J., Tedder, T.F., and Fearon, D.T. (1984) Identification of a 145,000 Mr membrane protein as the C3d receptor (CR2) of human B lymphocytes. *Proc Natl Acad Sci USA* **81:** 881–885.
Wiedemann, A., Linder, S., Grassl, G., Albert, M., Autenrieth, I., and Aepfelbacher, M. (2001) *Yersinia enterocolitica* invasin triggers phagocytosis via beta1 integrins, CDC42Hs and WASp in macrophages. *Cell Microbiol* **3:** 693–702.
Wright, S.D., and Jong, M.T. (1986) Adhesion-promoting receptors on human macrophages recognize *Escherichia coli* by binding to lipopolysaccharide. *J Exp Med* **164:** 1876–1888.
Wright, S.D., Tobias, P.S., Ulevitch, R.J., and Ramos, R.A. (1989) Lipopolysaccharide (LPS) binding protein opsonizes LPS-bearing particles for recognition by a novel receptor on macrophages. *J Exp Med* **170:** 1231–1241.
Wright, S.D., Ramos, R.A., Tobias, P.S., Ulevitch, R.J., and Mathison, J.C. (1990) CD14, a receptor for complexes of lipopolysaccharide (LPS) and LPS binding protein. *Science* **249:** 1431–1433.
Yamashita, S., Lukacik, P., Barnard, T.J., Noinaj, N., Felek, S., Tsang, T.M., *et al*. (2011) Structural insights into Ail-mediated adhesion in *Yersinia pestis*. *Structure* **19:** 1672–1682.
Yang, Y., Merriam, J.J., Mueller, J.P., and Isberg, R.R. (1996) The *psa* locus is responsible for thermoinducible binding of *Yersinia pseudotuberculosis* to cultured cells. *Infect Immun* **64:** 2483–2489.
Ye, Z., Kerschen, E.J., Cohen, D.A., Kaplan, A.M., van Rooijen, N., and Straley, S.C. (2009) Gr1+ cells control growth of YopM-negative *Yersinia pestis* during systemic plague. *Infect Immun* **77:** 3791–3806.
Ye, Z., Uittenbogaard, A.M., Cohen, D.A., Kaplan, A.M., Ambati, J., and Straley, S.C. (2011) Distinct $CCR2^{+}$ $Gr1^{+}$ cells control growth of the *Yersinia pestis* Δ*yopM* mutant in liver and spleen during systemic plague. *Infect Immun* **79:** 674–687.
Young, V.B., Falkow, S., and Schoolnik, G.K. (1992) The invasin protein of *Yersinia enterocolitica*: internalization of invasin-bearing bacteria by eukaryotic cells is associated with reorganization of the cytoskeleton. *J Cell Biol* **116:** 197–207.

Supporting information

Additional Supporting Information may be found in the online version of this article at the publisher's web-site:

Fig. S1. Flow cytometry gating scheme. All cells were stained with CCF2-AM and propidium iodide (PI). To identify lymphoid populations, cells were stained with a cocktail anti-CD19, anti-CD4, anti-CD8 and anti-NK1.1. To identify myeloid populations, cells were stained with a cocktail of anti-GR1, anti-CD11c, anti-CD11b and anti-MHC class II. Analysis began by gating on whole cells in a FSC-A vs. SSC-A plot. Whole cells were sent to a FSC-A vs. FSC-H plot to separate doublets and aggregates. Single cells were sent to a PI vs. FSC-A plot to separate live and dead cells. Live cells were then used for further analysis. For the lymphoid panel, live cells were sent to a CD8 vs. CD4 plot to identify T-cells. The double-negative population was then sent to a NK1.1 vs. CD19 gate to identify B-cells and NK cells. For the myeloid panel, live cells were sent to a GR1 vs. SSC-A plot to identify neutrophils and eosinophils. The remaining cells were then sent to a CD11c vs. MHC-II gate to identify dendritic cells. The double-negative populations were sent to a GR1 vs. CD11b plot to identify macrophages and monocytes. To calculate which cells had been injected ('frequency of injection'), either the total live cell population or the individual cell types were then sent to a blue vs. green plot. To determine the proportion of each cell type within the blue population ('blue cell distribution'), live cells were sent to the blue vs. green plot, and then blue cells were subjected to the myeloid or lymphoid analysis to identify cell types within the blue population.

Fig. S2. Analysis of total splenocytes from infected mice. Mice described in Fig. 1 were infected with either WT (panel A) or *Δail* (panel B) *Y. pestis*, and splenocyte populations were identified (described in Supporting Information Fig. S1). Changes in splenocyte populations according to bacterial burden are shown. Data were analysed by two-way ANOVA with Bonferroni multiple comparisons test to determine significant differences between uninfected controls compared with CFU categories for each cell type. ($^{*}P < 0.05$, $^{**}P < 0.01$, $^{***}P < 0.001$) DC, dendritic cells; Mac, macrophages; Mono, monocytes; Neut, neutrophils; Eosin, eosinophils; CD4, T helper cells; CD8, T cytotoxic cells; NK, NK cells.

Fig. S3. Representative analysis of flow cytometry data from *in vivo* infections. The data shown are from *in vivo* experiments with WT *Y. pestis* shown in Figs 1 and 2, but only data from the 10^{7} CFU category are shown here. The flow cytometry data analysis is described in Supporting Information Fig. S1. (A) After cell types are identified from total live cells, the % of blue cells in each population is determined. We refer to this as the 'Frequency of injection'. (B) Blue cells are first identified from total live cells and then subjected to the myeloid and lymphoid analysis to identify cell types within the blue population. We refer to this as the 'Blue cell distribution'. (C) Total live cells are subjected to the myeloid and lymphoid analysis to identify cell types within the total live cell population. This includes both uninjected (green) and injection (blue cells). We refer to this as the 'Total cell distribution'. (D) The blue cell distribution is compared with the total cell distribution. The fold difference for each cell type is shown above the pairs of bars. We refer to this difference as 'targeting efficiency'. (E) The targeting efficiency values are graphed to visualize which cells are enriched in the blue population compared with their proportion in the total splenocyte mixture (horizontal line at $Y = 1$ indicates no cell preference).

Fig. S4. Representative analysis of flow cytometry data from *ex vivo* infections. The data shown are from an infection of splenocytes with WT *Y. pestis* at an MOI of 1 in the absence of mouse serum. The flow cytometry data analysis is described in Supporting Information Fig. S2. (A) After cell types are identified from total live cells, the % of blue cells in each population is determined. We refer to this as the 'Frequency of injection'. (B) Blue cells are first identified from total live cells and then subjected to the myeloid and lymphoid analysis to identify cell types within the blue population. We refer to this as the 'Blue cell distribution'. (C) Total live cells are subjected to the myeloid and lymphoid analysis to identify cell types within the total live cell population. This includes both uninjected (green) and injection

(blue cells). We refer to this as the 'Total cell distribution'. (D) The blue cell distribution is compared with the total cell distribution. The fold difference for each cell type is shown above the pairs of bars. We refer to this difference as 'targeting efficiency'. (E) The targeting efficiency values are graphed to visualize which cells are enriched in the blue population compared with their proportion in the total splenocyte mixture (horizontal line at $Y = 1$ indicates no cell preference).

Fig. S5. Adhesin mutants have no defect in translocation in standard *ex vivo* infections. Splenocytes from naive mice were infected at an MOI of 1 with the indicated *Y. pestis* strains expressing YopM-Bla or Gst-Bla (not shown). Infections were performed in standard RPMI containing FBS and cytochalasin D for 1.5 h. Cells were stained with CCF2-AM and antibodies and then analysed by flow cytometry. The targeting efficiency for each cell type is shown (horizontal bar at $Y = 1$ indicates no cell preference). Data were analysed using two-way ANOVA with Bonferroni multiple comparisons test to determine significant differences for each cell type infected with WT compared with the mutant ($^{*}P < 0.05$, $^{**}P < 0.01$, $^{****}P < 0.0001$). DC, dendritic cells; Mac, macrophages; Mono, monocytes; Neut, neutrophils; Eosin, eosinophils; CD4, T helper cells; CD8, T cytotoxic cells; NK, NK cells.

Fig. S6. Target cell preference is adhesin independent. Splenocytes from naive mice were infected at an MOI of 1 with the indicated *Y. pestis* strains expressing YopM-Bla or Gst-Bla (not shown). Infections were performed in standard RPMI containing FBS, cytochalasin D and NMS for 1.5 h. Cells were stained with CCF2-AM and antibodies, and then analysed by flow cytometry. (A and C) The percentage of blue cells for individual cell types is shown. (B and D) The targeting efficiency for each cell type is shown (horizontal line at $Y = 1$ indicates no cell preference). Data were analysed using two-way ANOVA with Bonferroni multiple comparisons test to determine significant differences for each cell type infected with WT compared with the mutant. ($^{*}P < 0.05$, $^{***}P < 0.001$, $^{****}P < 0.0001$) DC, dendritic cells; Mac, macrophages; Mono, monocytes; Neut, neutrophils; Eosin, eosinophils; CD4, T helper cells; CD8, T cytotoxic cells; NK, NK cells.

Fig. S7. Target cell selection is not determined by bacterial adhesion. Splenocytes were infected with indicated *Y. pestis* strains expressing GFPuv. Infections were performed in RPMI containing FBS, cytochalasin D, and where indicated, NMS or IMS was added. Cells were stained with antibodies and analysed by flow cytometry to identify cell types and determine which cells had associated bacteria (GFP+). (A) The percentage of total splenocytes that are GFP+ is shown. (B) The comparison between WT and Δ*ail* infections in the presence of NMS is shown. (C) The effect of NMS on WT infection is shown. (D) The effect of NMS on Δ*ail* infection is shown. Data were analysed using two-way ANOVA with Bonferroni multiple comparisons test to determine significant differences for each cell type (white bars compared with black bars). ($^{*}P < 0.05$, $^{**}P < 0.01$, $^{***}P < 0.001$, $^{****}P < 0.0001$) DC, dendritic cells; Mac, macrophages; Mono, monocytes; Neut, neutrophils; Eosin, eosinophils; CD4, T helper cells; CD8, T cytotoxic cells; NK, NK cells.

Fig. S8. Blocking of host receptors requires serum factors. Splenocytes were left untreated (no Ab) or incubated with antibodies against CD14, CD11b and CD11c (+ Ab mix) prior to infecting with WT *Y. pestis* expressing YopM-Bla or Gst-Bla (not shown). Infections were performed in RPMI containing FBS, cytochalasin D and with or without 10% NMS. Cells were stained with CCF2-AM and antibodies to identify cell types, and then analysed by flow cytometry. (A) The targeting efficiency for wild-type infection is shown (B) The targeting efficiency for Δ*ail/pla/psaA* mutant infection is shown. Horizontal line at $Y = 1$ indicates no cell preference. two-way ANOVA with Bonferroni multiple comparisons test to determine significant differences for each cell type pretreated with Ab mix compared with the untreated control. ($^{****}P < 0.0001$) DC, dendritic cells; Mac, macrophages; Mono, monocytes; Neut, neutrophils; Eosin, eosinophils.